Biological Journal of the Linnean Society, 2023, **XX**, 1–24. With 5 figures.

Mitochondrial, morphological and environmental data partially support current subspecies designation in *Amazilia yucatanensis* hummingbirds

ANTONIO ACINI VÁSQUEZ-AGUILAR[1,2], M. CRISTINA MACSWINEY G. [2], FLOR RODRÍGUEZ-GÓMEZ[3] and JUAN FRANCISCO ORNELAS[1*]

[1]*Departamento de Biología Evolutiva, Instituto de Ecología, A.C. (INECOL), Carretera antigua a Coatepec No. 351, El Haya, Xalapa, Veracruz 91073, Mexico*
[2]*Centro de Investigaciones Tropicales (CITRO), Universidad Veracruzana, Xalapa, Veracruz, Mexico*
[3]*Centro Universitario de Ciencias Exactas e Ingenierías (CUCEI), Universidad de Guadalajara, Guadalajara, Jalisco, Mexico*

Received 7 October 2022; revised 7 December 2022; accepted for publication 19 December 2022

Historical geological events and Pleistocene climatic fluctuations have played important roles in shaping distribution and population differentiation across taxa. The buff-bellied hummingbird (*Amazilia yucatanensis*) is widely distributed along the Gulf of Mexico slope and the Yucatan Peninsula. Here, we obtained measurements and sequenced two mitochondrial DNA fragments from currently recognized subspecies: *Amazilia yucatanensis yucatanensis* (YUC), *Amazilia yucatanensis cerviniventris* (CER) and *Amazilia yucatanensis chalconota* (CHA). Additionally, we tested for their genetic and morphological differentiation, demographic expansion, palaeoclimatic distribution and niche overlap. Our results reveal genetic differentiation between two groups of populations: (1) from the Yucatan Peninsula to Veracruz (YUC+CER); and (2) from Veracruz to Tamaulipas (CHA). Neutrality tests and Bayesian skyline plots suggest past demographic expansion without changes in the effective population size over time. The potential distribution was fragmented at the Trans-Mexican Volcanic Belt and expanded northwards during the Last Glacial Maximum and Mid-Holocene to current conditions. Niche overlap was higher between YUC and CER. The environmental space occupied by subspecies was more similar to each other than expected by chance but significantly non-equivalent. Our results provide new insight on the distribution of this widespread hummingbird species and suggest that fragmentation during glaciations and differences in habitat have played a role in the recent diversification.

ADDITIONAL KEYWORDS: *Amazilia* – Mesoamerica – Mexico – mitochondrial DNA – niche divergence – Pleistocene – subspecies – Trans-Mexican Volcanic Belt – Trochilidae.

INTRODUCTION

Patterns of species genetic differentiation and genetic structure vary across taxa within the Mesoamerican region. This variation seems to be correlated with the ecological preferences of species and the dynamic landscape of the region. For taxa distributed in the highlands, a marked geographical structure of genetic variation and low levels of gene flow have been observed, with genetically distinct lineages corresponding to populations occurring in naturally isolated montane forests (McCormack *et al.*, 2011; Ruiz-Sanchez & Specht, 2013; Ornelas & González, 2014; Maldonado-Sánchez *et al.*, 2016; Ornelas *et al.*, 2016a; Zamudio-Beltrán & Hernández-Baños, 2018; Venkatraman *et al.*, 2019) or to those separated by major biogeographical barriers, such as the Isthmus of Tehuantepec, the Motagua–Polochic–Jocotán fault system and the Nicaraguan Depression (González *et al.*, 2011; Gutiérrez-Rodríguez *et al.*, 2011; Gutiérrez-García & Vázquez-Domínguez, 2012; Rodríguez-Gómez *et al.*, 2013; Ornelas & Rodríguez-Gómez, 2015; Zamudio-Beltrán *et al.*, 2020a, b). In contrast, for species that inhabit other environments or for those at lower elevations, low geographical structuring of genetic variation, high levels of gene flow and signs of

*Corresponding author. E-mail: francisco.ornelas@inecol.mx

recent population expansion have been found (Cavers *et al.*, 2003; Ramírez-Barahona & Eguiarte, 2014; Ornelas *et al.*, 2016b; Licona-Vera *et al.*, 2018b; Ortiz-Rodríguez *et al.*, 2020). The apparent discordance in the demographic and phylogeographical patterns suggests that the Mesoamerican taxa could have responded idiosyncratically to stochastic effects owing to extrinsic factors (i.e. broad spatial and temporal scales of geological and historical events, such as past climate changes; e.g. Ornelas *et al.*, 2013, 2015). However, an adherence to generic null expectations of concordance with reduced predictive power might limit explanations for discordant phylogeographical patterns of co-distributed taxa attributed to the idiosyncrasies of history and species-specific traits (Papadopoulou & Knowles, 2016).

Phylogeography has proved successful in explaining the impact of biogeographical barriers, geological events or past environmental change on the present distribution of genetic variation in hummingbirds. A growing number of phylogeographical studies have linked the impact of biogeographical barriers and Pleistocene glacial–interglacial cycles on current intraspecific genetic variation of hummingbird species in Mexico and Central America. Geographical structuring of genetic variation is observed in species with populations separated by biogeographical barriers (Rodríguez-Gómez *et al.*, 2013, 2021; Malpica & Ornelas, 2014; Rodríguez-Gómez & Ornelas, 2014; Jiménez & Ornelas, 2016; Hernández-Soto *et al.*, 2018; Zamudio-Beltrán *et al.*, 2020a, b), in species with disjunct distribution of populations (González *et al.*, 2011; Licona-Vera & Ornelas, 2014) or in those inhabiting naturally fragmented habitats, such as cloud forests (Cortés-Rodríguez *et al.*, 2008; Ornelas *et al.*, 2016a; Zamudio-Beltrán & Hernández-Baños, 2018). In contrast, low levels of geographical structuring, demographic expansion and high levels of gene flow across geographical barriers are observed among species inhabiting other habitats (Miller *et al.*, 2011; Rodríguez-Gómez & Ornelas, 2015, 2018; González-Rubio *et al.*, 2016; Licona-Vera *et al.*, 2018a).

A comparative study of past distribution models and phylogeographical data for eight hummingbird species distributed in the region indicated that the responses of these hummingbirds were idiosyncratic in the transition from the Last Interglacial (LIG) to the Last Glacial Maximum (LGM) and from the LGM to present conditions (Ornelas *et al.*, 2015). However, the geographical ranges of range-restricted species were more unstable over longer periods of time in comparison to widely distributed species, and within-population genetic variation decreased as populations were subjected to the transitions from the LIG to the LGM or from the LGM to the present (Ornelas *et al.*, 2015). However, the studied species are not strictly co-distributed, and they vary in several traits, including body size, heterogeneity of their environments across space, and their dispersal capacity across habitats.

Here, we focus on the buff-bellied hummingbird (*Amazilia yucatanensis* Cabot, 1845), a species widespread in the lowlands of the Gulf of Mexico slope and in those of the Yucatán Peninsula (Fig. 1). Three subspecies are recognized on the basis of geographical distribution and plumage colour variation (*Amazilia yucatanensis yucatanensis*, *Amazilia yucatanensis cerviniventris* and *Amazilia yucatanensis chalconota*). Specifically, we estimated the population structure and genetic relationships among recognized subspecies of *A. yucatanensis* using sequences of mitochondrial DNA (mtDNA), morphological data, ecological niche modelling and niche divergence tests. We asked (1) whether the genetic, morphological and ecological variation corresponds to existing subspecies and known geographical barriers; (2) whether divergence and demographic changes correspond temporally to the effects of historical events or Pleistocene glacial cycles; and (3) whether the current distribution of *A. yucatanensis* was triggered by historical habitat changes. Given that the environments of *A. yucatanensis* are heterogeneous across its geographical range and that potential climatic and/or geographical barriers to gene flow or the permeability of the landscape for passage of *A. yucatanensis* might have changed over time, we expect a weak pattern of genetic structuring and extensive gene flow and admixture across its distribution. Also, according to observed patterns for widespread hummingbird species in Mesoamerica, we expect that the palaeodistribution of *A. yucatanensis* populations contracted and fragmented during the LGM, whereas during the interglacials the distribution of populations expanded, allowing gene flow among populations and subspecies and, thus, erasing genetic structuring linked to contraction and fragmentation of suitable habitat during the LGM.

MATERIAL AND METHODS

Study system

The buff-bellied hummingbird (*A. yucatanensis*) is distributed on the slope of the Gulf of Mexico, from south Texas (lower Rio Grande Valley) and Tamaulipas through eastern Mexico to the Yucatán Peninsula, Chiapas, north-west Guatemala and north Belize (Friedmann *et al.*, 1950; Howell & Webb, 1995; Schuchmann, 1999; Vásquez-Aguilar *et al.*, 2021). Although sexes are similar in plumage coloration, the bill of males is bright red with a black tip, whereas in females it is mostly blackish above and red with a black tip below (Howell & Webb, 1995;

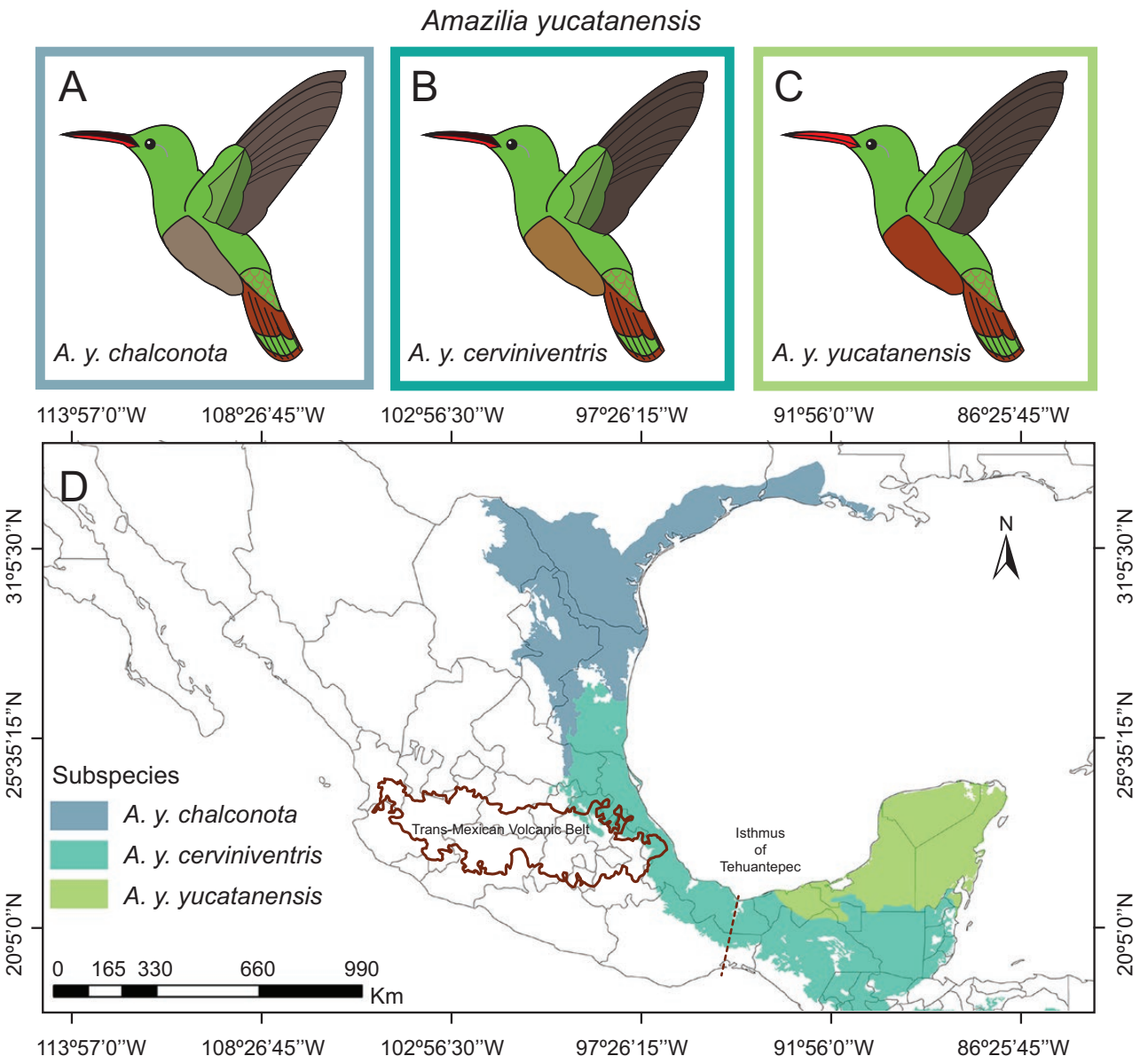

Figure 1. A, *Amazilia yucatanensis chalconota*. B, *Amazilia yucatanensis cerviniventris*. C, *Amazilia yucatanensis yucatanensis*. D, geographical distribution of *Amazilia yucatanensis* recognized subspecies on a map. The distribution areas were drawn according to Vásquez-Aguilar *et al.* (2021).

Fig. 1). It inhabits different types of environments, including seasonally deciduous tropical dry forest, sub-humid forest, bushes and scrubs from almost sea level to 1200 m a.s.l. (Howell & Webb, 1995). Three subspecies are currently recognized based on differences in distribution and plumage coloration, with the belly varying from pale greyish buff to cinnamon (Howell & Webb, 1995; Dickinson & Remsen, 2013; Chávez-Ramírez & Moreno-Valdéz, 2020; Fig. 1): *A. y. yucatanensis* (Cabot, 1845) is distributed on the Yucatán Peninsula south to east Tabasco, north-west Guatemala and north Belize (Fig. 1); *A. y. cerviniventris* (Gould, 1856) is distributed in eastern Mexico from central Veracruz south through Puebla and east Oaxaca to north Chiapas (Fig. 1); and *A. y. chalconota* Oberholser, 1898 is distributed from south Texas south to north Veracruz (north-eastern Veracruz, San Luis Potosí, Tamaulipas and Nuevo León; Fig. 1), recently extending its distribution north-east along the Gulf of Mexico coast, reaching Louisiana, Mississippi and Florida (Friedmann *et al.*, 1950; Schuchmann, 1999; Brush *et al.*, 2020; Chávez-Ramírez & Moreno-Valdéz, 2020; Vásquez-Aguilar *et al.*, 2021). Bent (1940) stated that *A. yucatanensis* is

not regularly migratory over most of its range, except for birds in the lower Rio Grande valley of Texas and Tamaulipas, Mexico. It appears, however, that after breeding, some individuals disperse north and north-east; in the Texas coastal bend south to south Texas, the species is rare from October to March, but it is somewhat more prevalent along the upper Texas coast and in Louisiana, Alabama and, occasionally, Florida (Chávez-Ramírez & Moreno-Valdéz, 2020). Numbers in all these regions are low, however; therefore, it seems likely that many individuals from south Texas and north-east Mexico migrate south in autumn and winter (Johnsgard, 1983). The validity of *A. y. chalconota* has been questioned, and its southern limits are unclear; although breeding individuals from San Luis Potosi are identified as *A. y. cerviniventris*, typical *A. y. chalconota* or intermediates occur in other seasons (Friedmann *et al.*, 1950).

Sample collection and DNA sequencing

For molecular analysis, we sampled 69 individuals (Supporting Information, Table S1) from 15 sites across the distribution of *A. yucatanensis* in Mexico and categorized them into three groups of sampling locations based on the geographical distribution of subspecies (*A. y. yucatanensis* = 5, YUC; *A. y. cerviniventris* = 7, CER; and *A. y. chalconota* = 3, CHA; Fig. 1; Supporting Information, Table S1). The sampling presented in this study covers most of the distribution of *A. yucatanensis*. Hummingbirds were captured using mist nets, and two rectrices were collected from each hummingbird as a source of DNA for subsequent genetic analysis (Harvey *et al.*, 2006) before the bird was released. Samples were collected under the required permits and using approved animal welfare protocols (see Acknowledgements).

Genomic DNA was extracted from tail feathers with the DNeasy blood and tissue extraction kit (Qiagen, Valencia, CA, USA), following the protocol recommended by the manufacturer. We amplified and sequenced three gene regions: NADH nicotinamide dehydrogenase subunit 2 (*ND2*, 388 bp) and the mitochondrial adenosine triphosphatase synthase 6 and 8 genes (*ATPase* 6 and 8, 720 bp). Amplification of *ND2* was conducted with the primers L5215 and H5578 (Hackett, 1996), whereas for the *ATPase* we used the primers L8929 (Sorenson *et al.*, 1999) and H9855 (Eberhard & Bermingham, 2004). The 12 µL polymerase chain reaction (PCR) mix for both fragments contained a final concentration of 0.72× PCR buffer (Promega, Madison, WI, USA), 3.6 mM $MgCl_2$, 0.58 mM deoxyribonucleotide triphosphates, 0.4 µg/µL bovine serum albumin, 0.18 µM of each primer, 0.04 U of Taq polymerase (Promega), 2 µL of genomic DNA and, finally, distilled H_2O added to make up the volume. The PCR conditions for *ND2* consisted of an initial denaturation at 94 °C for 2 min, followed by 35 cycles of denaturation at 94 °C for 30 s, annealing at 47 °C for 45 s and extension at 72 °C for 1 min, with a final extension at 72 °C for 10 min. For the *ATPase*, the PCR conditions consisted of an initial denaturation at 95 °C for 2 min, followed by 40 cycles consisting of denaturation at 92 °C for 40 s, annealing at 48–56 °C for 1 min and extension at 72 °C for 2 min, with a final extension at 72 °C for 10 min.

The PCR products were visualized on 1.5% agarose gels stained with GelRed (Biotium) and were purified using the QIAquick PCR purification kit (Qiagen), following the protocol recommended by the manufacturer. The purified DNA was sequenced in both directions using the BigDyeTM Terminator v.3.1 Cycle Sequencing kit (Applied Biosystems, Ann Arbor, MI, USA). Sequences were analysed on a 310 automated DNA sequencer (Thermo Fisher Scientific, Carlsbad, CA, USA) at the Institute of Ecology, A.C. (INECOL). Finally, the assembled sequences were edited manually and aligned with PhyDE (phylogenetic data editor) v.0.9971 (Müller *et al.*, 2006).

Relationships among haplotypes

Statistical parsimony networks for the single and concatenated mtDNA datasets were constructed to infer relationships among haplotypes as implemented in TCS v.1.2.1 (Clement *et al.*, 2000), with gaps treated as single evolutionary events and a 95% connection probability limit, and visualized using POPART v.1.7 (Leigh & Bryant, 2015). Loops were resolved following the criteria given by Pfenninger & Posada (2002). We downloaded the vouchered *A. yucatanensis* (LSUMZ_B-4090) *ND2* sequence from GenBank (accession no. KJ602180) and used it for *ND2* sequence alignment. We also took another approach for haplotype network construction, the haplotype median-joining network (Bandelt *et al.*, 1999) in POPART.

To examine the most likely number of genetically differentiated clusters without making a priori assumptions about the partitioning of genetic diversity, a Bayesian model-based approach was implemented in the program BAPS v.5.3 (Corander *et al.*, 2008) using the module for linked molecular data. For each marker, we surveyed the posterior probabilities (PP) of a different number of genetic clusters under the codon linkage model in two independent runs, with the number of proposed clusters (*K*) ranging from 2 to 15, with ten runs for each value of *K*.

Geographical structure and genetic diversity of populations

To test for the presence of hierarchical population structure, analyses of molecular variance (AMOVA) were run in ARLEQUIN v.3.5 (Excoffier & Lischer, 2010) using F_{ST} (among-population genetic variability) pairwise differences (Excoffier *et al.*, 1992). Populations (sampling locations) were treated as one group or grouped into two groups [(YUC+CER and CHA) or (YUC and CER+CHA)] or three groups (YUC, CER and CHA) corresponding to recognized subspecies (*A. y. yucatanensis*, *A. y. cerviniventris* and *A. y. chalconota*) (Supporting Information, Table S1). The significance of each AMOVA was determined with 10 000 permutations each. We also inferred the optimal number of geographically homogeneous and maximally differentiated groups (K) using a spatial analysis of molecular variance (SAMOVA) implemented in SAMOVA v.1.0 (Dupanloup *et al.*, 2002) and testing values of K ranging from two to nine, with ten replicates for each value of K. The configuration with the largest associated F_{CT} (among-group genetic variability) value was retained as the best grouping of populations. Locations with three samples or fewer were excluded from these analyses or lumped with closest location or corresponding subspecies (three samples from location 1 into population 2, one sample from location 7 into population 8, two samples from location 10 into population 12, and one sample from location 13 into population 14).

To describe intraspecific genetic variation of *A. yucatanensis*, molecular diversity indices (h, gene diversity; and π, nucleotide diversity), the diversity of segregating sites (θ) for each group of sampling locations, and pairwise comparisons of F_{ST} values between populations and groups of populations were calculated using ARLEQUIN v.3.5 (Excoffier & Lischer, 2010) with 1000 permutations. Haplotype diversity indices for each population (h_S, within-population-diversity and v_S, geographical average haplotype diversity) and at the species level (h_T, total diversity and v_T, geographical total haplotype diversity) and coefficients of population differentiation (G_{ST}, genetic differentiation for unordered alleles and N_{ST}, genetic differentiation for ordered alleles) were estimated using PERMUT v.2.0 (Pons & Petit, 1996). We also compared the G_{ST} and N_{ST} values and tested for phylogeographical structure using PERMUT with 10 000 permutations and the U-statistic. A value of N_{ST} significantly higher than the value of G_{ST} provides evidence of phylogeographical structure (Pons & Petit, 1996).

Demographic history

Signatures of demographic expansion in *A. yucatanensis* were addressed by means of neutrality tests, Fu's F_S (Fu, 1997), Tajima's D (Tajima, 1989) and Ramos-Onsins and Rozas' R_2 (Ramos-Onsins & Rozas, 2002) statistics of neutrality, and by conducting mismatch distribution analysis (Harpending, 1994) with ARLEQUIN. Significant negative values of D and F_S and small positive values of R_2 indicate an excess of low-frequency mutations relative to expectations under the standard neutral model (i.e. strict selective neutrality of variants, constant population size, and lack of subdivision and gene flow). Significance for R_2 was evaluated by comparing the observed values with null distributions generated by 10 000 replicates, using the empirical population sample size and the observed number of segregating sites in the 'pegas' package of R v.4.1.1 (Paradis, 2010; R Development Core Team, 2020). The mismatch distribution analysis was carried out in ARLEQUIN using the sudden demographic expansion model of Schneider & Excoffier (1999) in unsubdivided populations and the spatial expansion model in a subdivided population (Excoffier, 2004). We used 10 000 replicates to test the goodness of fit of the observed mismatch distribution to that expected under the spatial and sudden demographic expansion model using the sum of squares differences (SSD) and Harpending's raggedness index (Hri index; Harpending, 1994) according to Rogers & Harpending (1992). Low and non-significant values of Hri and SDD indicate a good fit between the observed and the expected values of the sudden expansion model (Rogers & Harpending, 1992).

Lastly, the time, t, at which the spatial expansion event took place was dated using the expression, $t = \tau/2\mu k$ (Schneider & Excoffier, 1999), where τ is the estimated number of generations since the expansion, μ is the mutation rate per site per generation, and k is the sequence length (*ND2* = 387 bp, *ATPase 6* = 516 bp, *ATPase 8* = 167 bp and combined mtDNA = 1108 bp). The time since expansion was estimated for each of the groups and using both the combined and partitioned mtDNA datasets and the geometric mean, 2.4287×10^{-2} substitutions per site per million years (s/s/Myr), of the mean substitution rates of *ND2* (2.9×10^{-2} s/s/Myr), *ATPase 6* (2.6×10^{-2} s/s/Myr) and *ATPase 8* (1.9×10^{-2} s/s/Myr) proposed by Lerner *et al.* (2011). The expansion parameter, τ, was estimated using ARLEQUIN in genetic lineages in which signs of sudden demographic expansion were evident. To convert the expansion parameter (τ) to real time since expansion in years (t), we used a generation time of 2.1 years, based on the observation that the age of maturity begins 1 year after hatching, and with an assumed low annual adult survival rate of 0.52 reported for *Basilinna* (= *Hylocharis*) *leucotis* (Ruiz-Gutiérrez *et al.*, 2012). The approximate average generation time (T) is calculated according to: $T = a + [s/(1 - s)]$ (Lande *et al.*, 2003), where a is the time to maturity, and s is the adult annual survival rate. Based on this, the estimate for T was 2.1 years.

Changes in the effective population size (N_e) through time were estimated using Bayesian skyline plots (BSPs) in BEAST v.2.6.4 (Drummond *et al.*, 2005; Drummond & Rambaut, 2007; Bouckaert *et al.*, 2014) for each group. This approach significantly improves the reliability of demographic inferences, because the power for detecting past population changes increases and the estimation error is substantially reduced (Ho & Shapiro, 2011). We chose the best nucleotide substitution model with empirical base frequencies using JMODELTEST v.2.0 (Darriba *et al.*, 2012), a strict clock model, and a piecewise linear coalescent Bayesian skyline tree prior with five starting groups. The HKY substitution model was the best model identified for YUC and CER, and HKY+I for CHA and when populations were treated as a single group. Two independent runs of 30 million generations each were run, with trees and parameters sampled every 3000 iterations and with a burn-in of 10%. The results of each run were visualized using TRACER (Rambaut *et al.*, 2018) to ensure that stationarity and convergence had been reached (effective sample size, ESS > 200). The time axis was scaled using the mtDNA geometric mean substitution rate of 0.01214 s/s/l/Myr (Lerner *et al.*, 2011).

MORPHOLOGY

Five body measurements were obtained from 105 hummingbirds (*A. y. yucatanensis* = 37 individuals; *A. y. cerviniventris* = 38 individuals; *A. y. chalconota* = 30 individuals) using a Mituyo dial calliper with a precision of 0.1 mm and a wing ruler: total body length (distance from the tip of the bill to the tip of the longest tail feather), wing chord (the distance from the carpal joint to the tip of the longest unflattened primary), exposed culmen (from the base of the bill to the tip of the upper mandible), bill width at the base of the upper mandible (at the anterior end of the nostrils) and tail length (from the uropygial gland to the tip of the longest rectrix). Measurements were taken on skin specimens by A.A.V.-A. and housed at the Colección de Aves del Instituto de Biología (IBUNAM) and at the Museo de Zoologia 'Alfonso L. Herrera' (MZFC), Facultad de Ciencias, Universidad Nacional Autónoma de México (UNAM).

Each specimen was assigned to subspecies (YUC, CER or CHA) by geography, and morphological data were tested for normality and $\log_{10}$-transformed ($x + 1$) before statistical analysis. We performed a principal components analysis (PCA) to explore morphological variation between *A. yucatanensis* subspecies in multivariate space and one-way ANOVAs to compare morphological differences between subspecies. Means (95% confidence intervals) of each group for each morphological trait were plotted and contrasted among groups using Tukey's post-hoc mean comparisons. All statistical analyses were performed in PAST v.4.03 (Hammer *et al.*, 2001).

ECOLOGICAL NICHE MODELLING

We used ecological niche modelling (ENM; Elith *et al.*, 2011) and constructed ENMs in MAXENT v.3.3.3k (Phillips *et al.*, 2006) with 19 bioclimatic variables from the WorldClim database (Hijmans *et al.*, 2005; Booth *et al.*, 2014) at a spatial resolution of ~1 km^2 (2.5 arc-min) to predict the present distribution of suitable habitat occupied by *A. yucatanensis* and during the Mid-Holocene (MH; ~6000 years ago; at 30 arc-seconds) and the LGM (~20 000 years ago; at 2.5 arc-minutes) past conditions based on CCSM4 and MIROC-ESM global models, and during the LIG (~120 000–140 000 years ago) at 30 arc-minutes spatial resolution (Hijmans *et al.*, 2005; Braconnot *et al.*, 2007). Coordinates of occurrence data were assembled mainly from online records in the public databases Global Biodiversity Information Facility [GBIF.org (17 June 2020) GBIF occurrence downloads; https://doi.org/10.15468/dl.xqs645], eBird (Sullivan *et al.*, 2009) and VertNet (http://portal.vertnet.org/search?q=Amazilia+yucatanensis), supplemented with our georeferenced records from field collection. Georeferenced data were checked for errors and data consistency for geographical coordinates. The dataset was verified spatially to remove duplicate points using SDM TOOLBOX v.2.2b in ARCMAP v.10.5 (ESRI, 2016), excluding duplicate occurrence records or those in close proximity to each other (~1 km^2) to reduce the effects of spatial autocorrelation. After careful verification of the location of every data point, excluding duplicate occurrence records, we restricted the dataset to 310 unique presence records for the analysis.

To exclude highly correlated variables and multicollinearity, we ran a Pearson correlation test among the 19 climatic variables for each dataset using the 'ggplot2' (Wickham, 2016) and 'corrplot' (Wei & Simko, 2017) libraries in R v.4.0.0 (R Development Core Team, 2020). When Pearson's correlation coefficients were > 0.8 the variables were considered highly correlated, whereas variables with correlation coefficients < 0.8 were selected to represent climatic limitations (Pearson *et al.*, 2007). However, we are aware that hazards of multicollinearity to the recommended > 0.7 threshold are possible (Dormann *et al.*, 2013). After removing highly correlated variables, six variables were used to generate the ENM in current climate conditions using MAXENT [BIO3 = isothermality, BIO4 = temperature seasonality (SD × 100), BIO7 = temperature annual range (BIO5 – BIO6), BIO13 = precipitation of wettest month, BIO15 = precipitation seasonality

and BIO17 = precipitation of driest quarter]. The ENMs were calibrated to delineate a realistic region of accessible areas for the species ('M'; BAM diagram; Soberón & Peterson, 2005), the set of sites accessible to a species over which models are calibrated (Soberón & Peterson, 2005; Barve *et al.*, 2011; Freeman *et al.*, 2019; Atauchi *et al.*, 2020) based on the ecoregions of eastern Mexico and Central America proposed by Olson *et al.* (2001), representing potential boundaries on the landscape to dispersal (Barve *et al.*, 2011), and the distribution of the species considering elevational range limits of *A. yucatanensis* (Barve *et al.*, 2011). After calibration, we masked all environmental variables to the extent of the 'M' in ArcMap (ESRI, 2016).

Final models for *A. yucatanensis* were constructed without extrapolation and with no clamping, in order to avoid artificial projections of extreme values of ecological variables (Elith *et al.*, 2011; Owens *et al.*, 2013; Prieto-Torres *et al.*, 2020), and other MaxEnt parameters were set to the default for convergence threshold (10^{-5}) and 500 iterations, ensuring only one locality per grid cell. The models were run with ten cross-validation replicates and with 30% of occurrence records for model evaluation, which is considered appropriate for estimating the probability of presence (Phillips *et al.*, 2017), using the tenth percentile training presence logistic threshold (T10LT). The averages of all runs were used as final models, and jackknife analysis was used to determine the factors contributing the greatest amount to habitat suitability (Borzée *et al.*, 2019). The obtained maps were subsequently converted into binary presence–absence data, and overlapping was performed in ArcMap v.10.5 (ESRI, 2016).

The final MaxEnt models were evaluated by calculating the area under the curve (AUC) of the receiver operating characteristic (ROC) curve (Elith *et al.*, 2011), a threshold-independent statistic varying from zero to one, in which values of ~0.5 represent distribution models no better than random and those close to one represent a perfect fit between the observed and predicted species distribution; acceptable models are those with AUC values > 0.7 (Phillips *et al.*, 2006). However, several criticisms have been associated with this approach (e.g. Lobo *et al.*, 2008; Merow *et al.*, 2014; Cobos *et al.*, 2019; Vásquez-Aguilar *et al.*, 2021), including that the two error components (omission and commission) are inappropriately weighted equally. Therefore, the statistical performance of the models was also evaluated using the partial ROC test (Peterson *et al.*, 2008). Within a value ranging from zero to two, values higher than one suggest a performance better than chance, by analysing the presence vs. the absence against the total area predicted by MaxEnt (Osorio-Olvera *et al.*, 2020).

The resulting species distribution in the present climate conditions was projected onto past climate scenarios at the LIG, LGM and MH [at 30 s of arc (arc s)], using MaxEnt. The LGM layers were resampled to 30 arc-s using the bi-linear method through the 'resample' package in R v.3.4.1. Past climate layers were drawn from the WorldClim webpage for the LIG (Otto-Bliesner *et al.*, 2006), and for the MH and LGM they were based on two global models (Braconnot *et al.*, 2007): the community climate system model (CCSM) (Collins *et al.*, 2004) and the model for interdisciplinary research on climate (MIROC) (Hasumi & Emori, 2004). The CCSM and MIROC climate models simulate different climate conditions, with cooler sea-surface temperature conditions assumed in CCSM than in MIROC, resulting in higher annual precipitation in CCSM than in MIROC (Otto-Bliesner *et al.*, 2007).

Niche divergence

We quantified the differentiation between climatic niches of *A. yucatanensis* mtDNA groups of populations (YUC, CER and CHA) based on their ENMs with ENMTools (Warren *et al.*, 2010). Climate niche overlaps among groups were estimated using the PCA-env method proposed by Broennimann *et al.* (2012), with the same six variables used to generate the ENM in the present climate conditions. Principal components analysis was used to transform the environmental space of the selected environmental variables into a two-dimensional space defined by the first and second principal components (Strubbe *et al.*, 2015). The PCA-env was carried out to transform the climate layers into a reduced number of linearly uncorrelated variables (i.e. principal components; Broennimann *et al.*, 2012). Subsequently, the overlapping of the niches by pairs of the groups was calculated using Schoener's *D* metric (Schoener, 1970). The values of this metric ranges from zero (meaning that the niches are completely different) to one (meaning that the niches completely overlap) (Broennimann *et al.*, 2012), and graphs were made to observe the surface density of occurrences for each group.

Two different randomization tests were used to test the niche evolution hypotheses (Broennimann *et al.*, 2012): an equivalency test, which determined whether the niches of two entities in two geographical ranges were equivalent (i.e. whether the niche overlap was constant, by randomly reallocating the occurrences of both entities between the two ranges); and a similarity test, which compared the niche overlap of one randomly distributed range on its background while keeping the other unchanged, then performed the reciprocal comparison. Each randomization process was repeated 100 times (to ensure that the null hypothesis could be rejected with a high level of confidence), producing a

null distribution of overlapping values against which the observed score was compared. If the observed value of *D* was located outside 95% of the density of the stochastically simulated (ss) values, the null hypothesis was rejected (H0 = the niches are similar or equivalent), which implied that the groups occupied different environmental spaces (Broennimann *et al.*, 2012). The ss values were generated using the ENM of each subspecies group and an ENM created with random points drawn from the minimum convex polygon surrounding the original occurrence records of the other genetic groups of *A. yucatanensis*. The geographical ranges of the genetic groups were used as backgrounds individually. For the background test, we used the minimum convex polygon surrounding the original occurrence records and the entirety of Mexico and Guatemala as the species range. All analyses were computed with the *ecospat* package (Di Cola *et al.*, 2017) in R v.4.1.1 (R Core Team, 2020) and ENMTools (Warren *et al.*, 2010).

RESULTS

Haplotype networks and spatial clustering

Statistical parsimony retrieved well-resolved haplotype networks (Fig. 2). The alignment of *ND2*, *ATPase* and concatenated *ND2* + *ATPase* genes yielded a total of 388, 720 and 1108 bp, with 10, 19 and 27 variable sites, respectively. Sequence alignment of samples from 16 localities yielded ten *ND2* (n = 70 including KJ602180) and 14 *ATPase* (n = 64) haplotypes, with different frequency across geography (Fig. 2A, B; Supporting Information, Table S2).

Twenty-one mtDNA haplotypes were recovered when sequences were concatenated (n = 64; Fig. 2C). Seven localities exhibited more than one haplotype (Supporting Information, Table S2). The statistical parsimony network of concatenated mtDNA sequence data retrieved a single network, in which two haplogroups (mtDNA groups) were revealed: *A. y. yucatanensis* + *A. y. cerviniventris* (YUC+CER) and *A. y. chalconota* (CHA) (Fig. 2D; Supporting Information, Table S2). Several mutational steps separated the two haplogroups, and no haplotype sharing was observed (Fig. 2D). Haplotype H14 formed the core of the first haplogroup (CHA; *A. y. chalconota*), which was composed of nine haplotypes (H13–H21) found exclusively in populations from Puebla to Tamaulipas (Fig. 2D). The second haplogroup was composed of two most frequent haplotypes (H6 and H11), three less frequent haplotypes (H1, H5 and H9), and seven singletons (H2–H4, H7, H8, H10 and H12); the most widespread haplotype, H11, was distributed exclusively in *A. y. cerviniventris* populations (CER), and the second most frequent haplotype, H6, was distributed exclusively in *A. y. yucatanensis* populations (YUC) (Fig. 2C, D; Supporting Information, Table S2). Both network estimation methods found essentially the same associations between haplotypes (Supporting Information, Fig. S1); however, in the median-joining network of combined mtDNA several ambiguous connections were detected (Supporting Information, Fig. S1).

The BAPS analyses with mtDNA sequences indicated the existence of two genetic clusters (K = 2) as the best partition (log marginal likelihood = −721.8109, PP = 1.0), suggesting a lack of genetic structure between *A. y. yucatanensis* and *A. y. cerviniventris* subspecies (Fig. 2E).

Geographical structure and genetic diversity of populations

The AMOVAs showed significant genetic differentiation at each hierarchical level (Table 1). When groups were not defined, the highest percentage of variation (81.8%) was explained by differences among populations and only 18.1% by differences within populations (Table 1). When grouping populations (sampling locations) into two groups (YUC+CER and CHA), population structure was highest and significant (F_{CT} = 0.78, P = 0.01; Table 1). When populations were grouped into three groups of populations or subspecies (YUC, CER and CHA), the genetic differentiation was also high and significant (F_{CT} = 0.75, $P < 0.001$; Table 1).

The SAMOVA detected strong geographical structure (F_{CT} = 0.77, $P < 0.001$), with same two groups of populations inferred (YUC+CER and CHA) as the optimal number of geographical clusters for K = 2 (Table 1). The AMOVA and SAMOVA results were similar when locations with three samples or fewer were excluded from these analyses (Supporting Information, Table S3).

The number of haplotypes varied among groups, from four in CER with 24 samples to nine in CHA with 17 samples (Table 2). Genetic diversity was highest for CHA, followed by YUC and CER, and nucleotide diversity was highest for YUC, followed by CHA and CER (Table 2). Differentiation among populations based on mtDNA variation (mean ± SE; G_{ST} = 0.632 ± 0.1016) indicated that *A. yucatanensis* is genetically subdivided. Genetic diversity across populations (h_T = 0.859 ± 0.0877; v_T = 0.860 ± 0.3112) was higher than the average within-population value (h_S = 0.316 ± 0.1032; v_S = 0.301 ± 0.2362). However, PERMUT analysis showed that N_{ST} and G_{ST} values were not significantly different (N_{ST} = 0.650 ± 0.1945 vs. G_{ST} = 0.632 ± 0.1016, permutation: 10 000, $P > 0.05$), indicating no phylogeographical structuring.

Pairwise comparisons of F_{ST} values were high and significant when sampling locations (Supporting

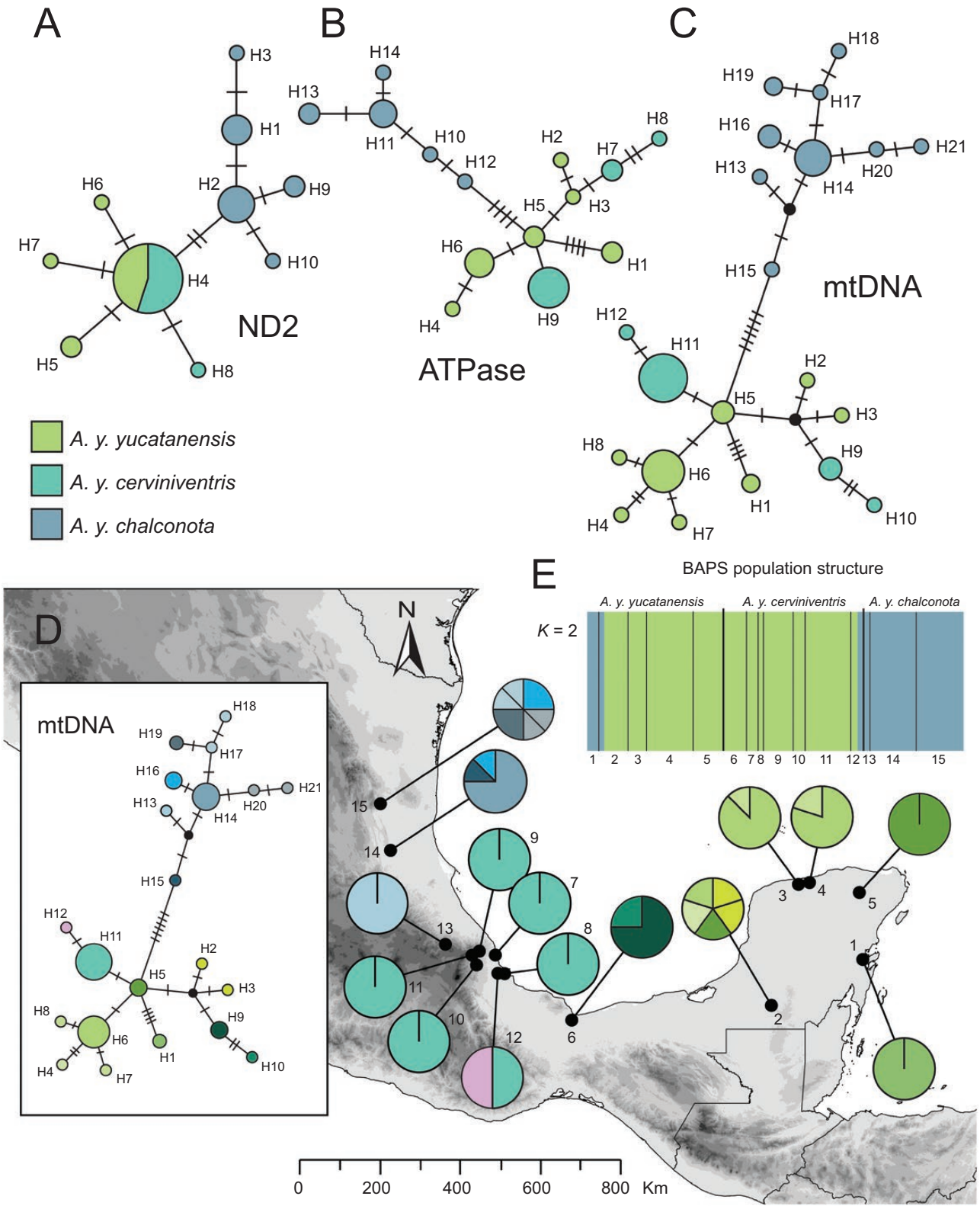

Figure 2. Statistical parsimony networks of *ND2* data (A), *ATPase* data (B) and combined *ND2* + *ATPase* (mtDNA) data (C) of *Amazilia yucatanensis*. D, mtDNA data of *Amazilia yucatanensis* overlaid on a map of northern Mesoamerica. Numbers correspond to sampling localities. See the Supporting Information (Appendix S1) for sampling locality information and

Table 1. Results of analysis of molecular variance (AMOVA) and spatial analysis of molecular variance (SAMOVA) models on *Amazilia yucatanensis* populations: (1) with no groups defined a priori; (2) grouped into two groups (YUC+CER and CHA); (3) grouped into two groups (YUC and CER+CHA); (4) grouped into three groups (YUC, CER and CHA) according to geographical distribution (Fig. 1; Supporting Information, Table S1); and (5) SAMOVA (K = 2)

	d.f.	Sum of squares	Estimated variance	Percentage	Fixation indices
1. No groups defined					
Among populations	10	135.345	2.27012	81.87	
Within populations	53	26.639	0.50263	18.13	F_{ST} = 0.81**
Total	63	161.984	2.77274		
2. Two groups					
Among groups	1	101.787	3.8727	78.06	F_{CT} = 0.78*
Among populations within groups	9	33.558	0.5856	11.80	F_{SC} = 0.53**
Within populations	53	26.639	0.5026	10.13	F_{ST} = 0.89**
Total	63	161.984	4.9610		
3. Two groups					
Among groups	1	30.082	0.5668	18.59	F_{CT} = 0.18 ns
Among populations within groups	9	105.263	1.9791	64.92	F_{SC} = 0.79**
Within populations	53	26.639	0.5026	16.49	F_{ST} = 0.83**
Total	63	161.984	3.0486		
4. Three groups					
Among groups	2	115.933	2.6074	75.30	F_{CT} = 0.75**
Among populations within groups	8	19.412	0.3525	10.18	F_{SC} = 0.41**
Within populations	53	26.639	0.5026	14.52	F_{ST} = 0.85**
Total	63	161.984	3.4625		
5. SAMOVA (K = 2)					
Among groups	1	101.787	3.8646	77.90	F_{CT} = 0.77**
Among populations within groups	8	33.508	0.6023	12.14	F_{SC} = 0.54**
Within populations	54	26.689	0.4942	9.96	F_{ST} = 0.90**
Total	63	161.984	4.9612		

Abbreviations: CER, *Amazilia yucatanensis cerviniventris*; CHA, *Amazilia yucatanensis chalconota*; YUC, *Amazilia yucatanensis yucatanensis*. F-statistics were used to estimate the proportion of genetic variability found among populations (F_{ST}), among populations within groups (F_{SC}) and among groups (F_{CT}): ns, not significant ($P > 0.05$), *$P < 0.05$ and **$P < 0.0001$.

Information, Table S4) or groups of populations (subspecies) were compared (YUC vs. CER, F_{ST} = 0.4388, $P < 0.001$; YUC vs. CHA, F_{ST} = 0.8650, $P < 0.001$; CER vs. CHA, F_{ST} = 0.8242, $P < 0.001$).

Demographic history

For *ND2 + ATPase*, Fu's F_S and Tajima's D values for *A. yucatanensis* groups of populations (YUC, CER and CHA) were, in most cases, negative and non-significant, indicating that populations were neutrally evolving (except the Fu's F_S value for CHA, which was negative and significantly different from zero; Table 2). In contrast, mismatch distributions and the low and non-significant SSD and Hri values indicated a good fit to the demographic expansion model and were consistent with a scenario of a sudden demographic expansion, except for the SSD of the YUC group (Table 2; Supporting Information, Fig. S2A). Finally, the R_2 statistic showed positive, small and highly significant values for YUC and CHA groups, indicating that these groups presented past demographic expansion (Table 2; Supporting Information, Fig. S2A). Based on our estimated values of τ, the average time since the demographic expansion was 36.87–8.58 kya BP for YUC, 502.74–117.09 kya BP for CER and 284.89–66.35 kya BP for CHA (Table 2).

The Bayesian skyline plots suggested that the effective population size was stable over time in the

haplotype distribution. Haplotypes are coded with a different colour according to the geographical regions of subspecies, and each of the haplotypes is indicated by a number. The size of segments of the pie charts corresponds to the number of individuals with that haplotype. In E, a Bayesian analysis of population genetic structure (BAPS) is presented based on the *ND2 + ATPase* sequences. Colours indicate different genetic clusters (K = 2).

Table 2. Diversity indices and summary statistics of demographic analysis of *Amazilia yucatanensis* samples by four groups (YUC, CER, CHA, and Global) resembling geographical history to infer demographic range expansion (Fig. 1; Supporting Information, Table S1)

Parameter	YUC	CER	CHA	Global
Mitochondrial DNA				
N	23	24	17	64
N_H	8	4	9	21
h	0.7115 ± 0.0924	0.3696 ± 0.1173	0.8603 ± 0.0684	0.8681 ± 0.0293
π	0.00166 ± 0.00111	0.00109 ± 0.00080	0.00152 ± 0.00105	0.00471 ± 0.00257
D	−1.33447	−0.91699	−0.24135	−0.31648
F_S	−2.18926	0.63566	**−4.81163***	−4.22820
SSD	0.31078**	**0.07213**	**0.01101**	**0.03025**
Hri	**0.04101**	**0.41916**	**0.09629**	**0.03025**
R_2	**0.0591****	0.0591	**0.0888***	**0.05***
t_1	8.59	117.09	66.35	195.54
t_2	36.87	502.74	284.89	138.41

Abbreviations: CER, *Amazilia yucatanensis cerviniventris*; CHA, *Amazilia yucatanensis chalconota*; D, Tajima's D; F_S, Fu's F_S; h, gene diversity; Hri, Harpending's raggedness index; N, number of individuals, N_H, number of haplotypes; π, nucleotide diversity R_2, Ramos-Onsins and Rozas' statistic; SDD, differences in the sum of squares or mismatch distribution; t_1, time since expansion (in kiloyears before present) for concatenated mtDNA; t_2, time since expansion (in kiloyears before present) for partitioned mtDNA; YUC, *Amazilia yucatanensis yucatanensis*.
Positive values of Tajima's D and F_S are indicative of mutation–drift–equilibrium, which is typical of stable populations, whereas negative values that result from an excess of rare haplotypes indicate that populations have undergone recent expansions, often preceded by a bottleneck. Significantly negative values (at the 0.05 level) in both tests reveal historical demographic expansion events. Significant ($P \leq 0.05$) values of SSD and Hri indicate deviations from the sudden expansion model. In bold are shown values that are consistent with demographic expansion. Small positive values of R_2 are expected under a scenario of population expansion.
*$P < 0.05$, **$P < 0.001$.

three subspecies, except for a marginal increase before the LGM when evaluated as a whole population or species (Supporting Information, Fig. S2B).

Morphological variation

We found morphological differences among *A. yucatanensis* subspecies. Principal components analysis reduced morphological measures to two PCs that explained 78.4% of the total variance: PC1 (59.5%) was explained largely by exposed culmen and PC2 (18.9%) determined mainly by tail length (Fig. 3A). Univariate ANOVAs showed significant differences among subspecies in total body length, exposed culmen and bill width (one-way ANOVAs: total body length, $F_{2,104} = 12.47$, $P < 0.001$; exposed culmen, $F_{2,104} = 21.14$, $P < 0.001$; bill width, $F_{2,104} = 6.91$, $P < 0.001$; wing chord, $F_{2,104} = 2.06$, $P > 0.05$; tail length, $F_{2,104} = 1.53$, $P > 0.05$). Overall, Tukey's post-hoc mean comparisons showed that individuals of the CHA group had significantly larger bills than YUC and CER and that the body length of the YUC group was significantly shorter than CHA and CER (Fig. 3B).

Ecological niche modelling

The present distribution model of *A. yucatanensis* was supported by high predictive power (Figs 4, 5A) that resulted in a better mean proportion of correctly classified training observations and yielded a good fit for the present geographical distribution of the species (mean ± SD; AUC = 0.787 ± 0.003). The partial ROC test (1.4709 ± 0.0896) showed that models were statistically significant ($P < 0.01$).

The LIG, LGM and MH distribution models yielded similar but somewhat more restricted conditions than the present distribution (Fig. 4). During the LIG, the projection of the models yielded a connected distribution of *A. yucatanensis*, but more restricted northwards than the prediction in the present distribution model, with a fragmented and expanded distribution northwards (Fig. 4). The projections to LGM and MH conditions showed a more contracted and fragmented distribution in both CCSM and MIROC models (Fig. 4). Overall, the estimated potential distribution of *A. yucatanensis* revealed fragmentation of suitable environmental conditions after the LGM, similar to its present distribution, potentially expanding their distribution on the Yucatán Peninsula and northwards during the LGM, particularly under the CCSM scenario, and fragmenting from the MH to present conditions at the Trans-Mexican Volcanic Belt (TMVB; Fig. 4).

Niche divergence

The PCA-env indicated that 84.61% of the environmental variation (19 bioclimatic variables)

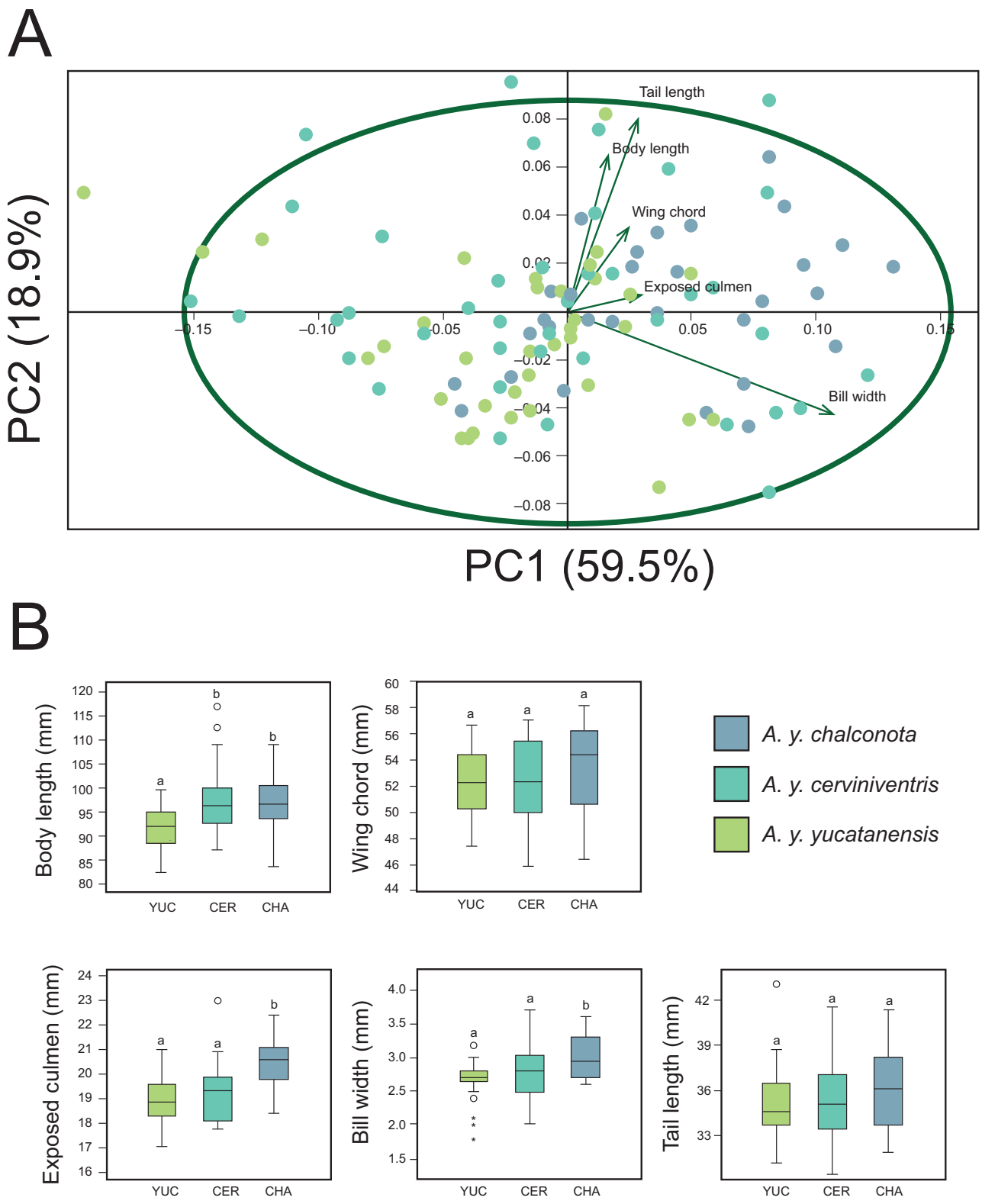

Figure 3. Morphological measurements (mean ± 1 SE) of *Amazilia yucatanensis* subspecies. *N* = sample size in parentheses. A, principal components analysis showing the first two principal components (PCs) explaining 78.4% of the total variation. (B) Boxplots of each morphometric character (total body length, wing chord, exposed culmen, width of bill and tail length) measured in millimetres.

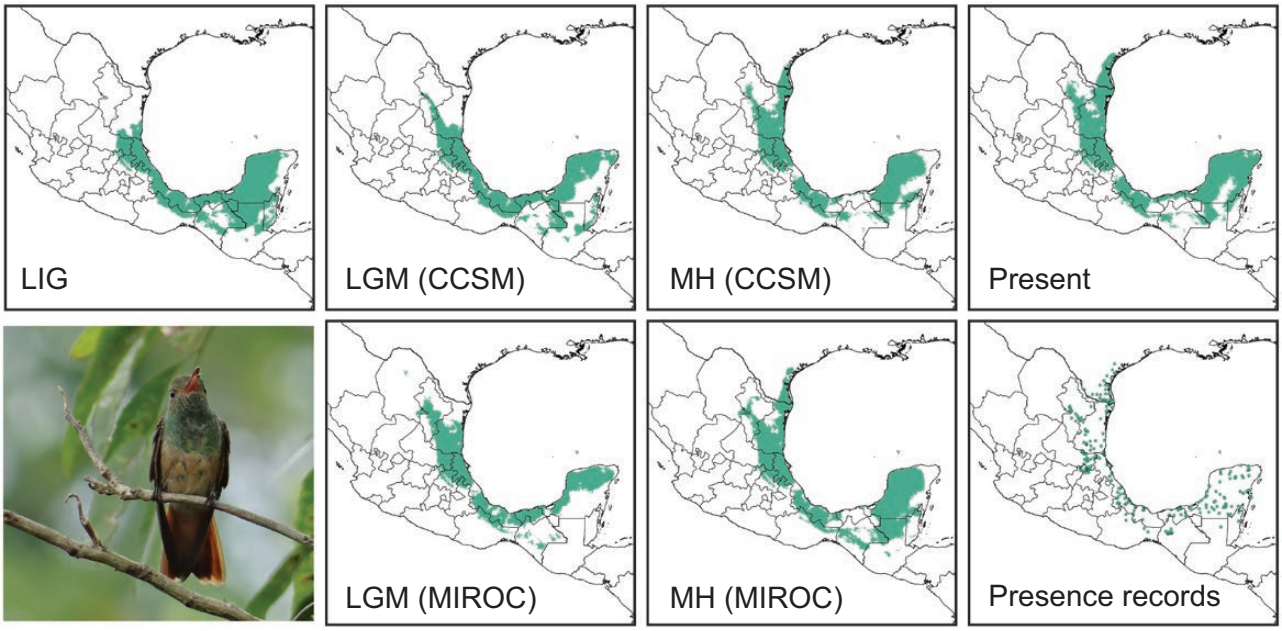

Figure 4. Species distribution models for *Amazilia yucatanensis* hummingbirds at the Last Interglacial (LIG; 140–120 kya), Last Glacial Maximum [LGM; 21 kya; community climate system model (CCSM) and model for interdisciplinary research on climate (MIROC)], Mid-Holocene (MH; 6 kya; CCSM and MIROC) and at present. Species distribution models are shown with the threshold value of equal training sensitivity and specificity. Green dots correspond to occurrence records used for modelling current species distribution. Photograph of Amazilia yucatanensis cerviniventris by Aurelio Molina Hernández.

was explained by the first two PCs (PC1, 60.52%; PC2, 24.09%; Fig. 5B). Principal component 1 was positively associated with temperature variables (BIO3 = isothermality and BIO7 = temperature annual range) and precipitation of the wettest month (BIO13) and negatively associated with precipitation variables (BIO15 = precipitation seasonality and BIO17 = precipitation of driest quarter), while the second niche axis (PC2) was positively associated with precipitation seasonality (BIO15) and negatively associated with mean temperature of wettest quarter (BIO4) (Supporting Information, Table S5).

The occurrence density surfaces in environmental space, as determined by PCA-env, showed that the position in environmental space varied among lineages. Each lineage differed in their position in environmental space (Fig. 5C–E). The contribution of the climatic variables to the two axes of the PCA-env and the percentage of inertia explained by the two axes are presented in the Supporting Information (Fig. S3). Niche overlap between *A. yucatanensis* genetic groups (YUC, CHA and CER) was low, with Schoener's *D* values < 0.2023 (Table 3), suggesting that subspecies occupy considerably more different environmental niches from each other than expected by chance. The niches occupied by the genetic groups were significantly non-equivalent ($P < 0.009$); the null hypothesis of niche equivalency was rejected for all comparisons between lineages (Table 3; Supporting Information, Fig. S3). For niche similarity tests, all comparisons were rejected, indicating that their environmental space is more similar to each other than expected by chance (Table 3; Supporting Information, Fig. S3).

DISCUSSION

AMAZILIA YUCATANENSIS HUMMINGBIRDS IN MESOAMERICA

In this study, we have elucidated the geographical structure of *A. yucatanensis* mtDNA sequence genetic variation in Mesoamerica and determined the effects of geographical barriers, the geographical distribution of suitable habitat and environmental variability on population divergence over time. The haplotype network for the combined mtDNA dataset, F_{ST} statistics, BAPS, AMOVA and SAMOVA estimates revealed the existence of two genetically distinct groups of populations (CHA and YUC+CER).

The presence of haplotypes private to each subspecies suggests that haplotypes are not closely related but geographically distributed by subspecies, partly supporting the current subspecies designation: *A. y. yucatanensis*, *A. y. cerviniventris* and *A. y. chalconota* (Schuchmann, 1999; Vásquez-Aguilar *et al.*, 2021). Furthermore, the AMOVA grouping the

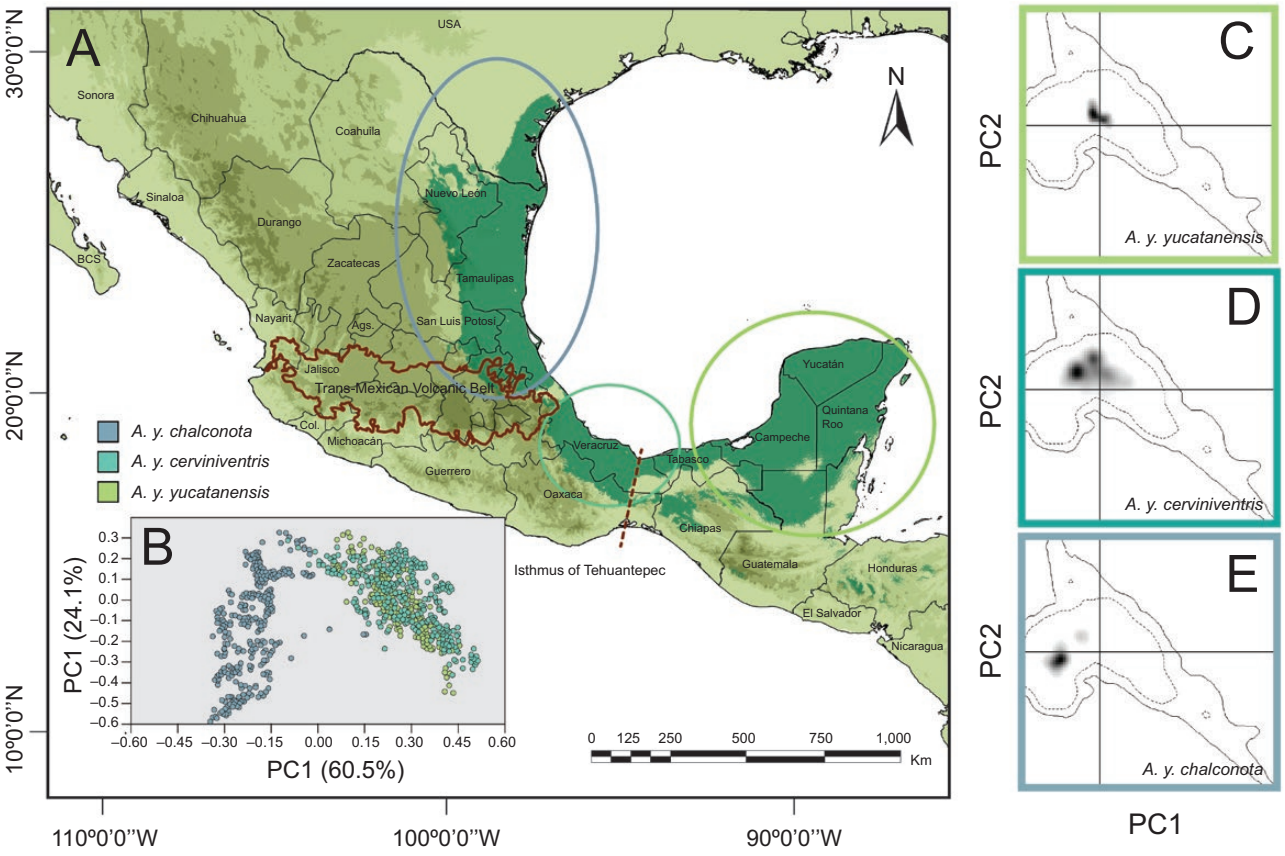

Figure 5. A, predicted distribution of *Amazilia yucatanensis* at present. B, principal components analysis on the bioclimatic variables for subspecies of *A. yucatanensis*. C–E, *Amazilia yucatanensis yucatanensis* (YUC; C), *Amazilia yucatanensis cerviniventris* (CER; D) and *Amazilia yucatanensis chalconota* (CHA; E) population niche displayed on the same multidimensional scale represented by the first two axes (PC1 and PC2) of a principal components analysis summarizing the entire study area. Grey shading shows the density of the occurrences of the species by cell. The continuous and dashed contour lines illustrate 100% and 50% of the available (background) environment, respectively.

Table 3. Ecological niche comparisons for the *Amazilia yucatanensis* genetic groups

Comparisons		Niche overlap (*D*)	Niche similarity		Niche equivalency
a	*b*		$a \rightarrow b$	$b \rightarrow a$	
YUC	CER	0.2023	Similar	Similar	Non-equivalent**
CER	CHA	0.0776	Similar	Similar	Non-equivalent**
YUC	CHA	0.0047	Similar	Similar	Non-equivalent**

Abbreviations: CER, *Amazilia yucatanensis cerviniventris*; CHA, *Amazilia yucatanensis chalconota*; YUC, *Amazilia yucatanensis yucatanensis*.
Pairwise niche overlap values are presented for the comparisons of niche similarity and equivalency of species *a* with species *b* in terms of Schoener's *D*, niche similarity *P*-values and equivalency via randomization test. The ecological niches are significantly more similar than expected by chance (niche similarity test) or more equivalent than expected by chance (niche equivalency test).
$^{**}P < 0.01$.

sampling locations into three groups of populations (YUC, CER and CHA) or subspecies suggests restricted gene flow between the three geographical areas. Genetic diversity in both YUC and CER groups was high. However, haplotypes differ from each other by only one mutation in most cases, suggesting the recent formation and shallow differentiation between YUC and CER. The combination of high genetic diversity (h) and low nucleotide diversity (π) values also indicates rapid population growth from ancestral populations

with small effective population size (Avise, 2000). Although restricted gene flow between genetic groups might be indicative of allopatric fragmentation, the shallow genetic differentiation between YUC and CER could also result from non-sampled haplotypes from intermediate populations or from populations separated by long distances. Thus, increased population sampling along the Gulf of Mexico slope and within sampling gaps (between localities 1 and 2–3, between localities 2 and 6, and between localities 13 and 14; Fig. 2D) in combination with a niche modelling approach and nuclear DNA markers with higher resolution (microsatellites) are needed for further assessment of the hypothesis of allopatric fragmentation and the evolutionary distinctiveness and subspecies status of these two mtDNA genetic groups of *A. yucatanensis*.

Our results suggest the existence of two mtDNA genetic groups (CHA and YUC+CER) associated with geography, separated by the TMVB. Some hummingbird species migrate across large distances and geographical barriers (e.g. Russell *et al.*, 1994; Malpica & Ornelas, 2014; Licona-Vera *et al.*, 2018a) or wander from the lowlands up to the cloud and temperate forests during the non-breeding season and vice versa (Johnsgard, 1983; Rodríguez-Gómez & Ornelas, 2015; Hernández-Soto *et al.*, 2018; Zamudio-Beltrán *et al.*, 2020a, b; Rodríguez-Gómez *et al.*, 2021), allowing for gene flow among populations. Thus, the observed genetic differentiation among *A. yucatanensis* populations linked to the TMVB, as a physical barrier, was unexpected.

Phylogeographical structure along the TMVB, a magmatic arc of ~8000 volcanic structures, has been documented in several plant and vertebrate species (Parra-Olea *et al.*, 2012; Velo-Anton *et al.*, 2013; Kingston *et al.*, 2014; Ruiz-Sanchez & Specht, 2014; Pérez-Crespo *et al.*, 2017; Bryson *et al.*, 2021; Cisneros-Bernal *et al.*, 2022). The strong climatic fluctuations between glacial and interglacial periods during the Pleistocene probably shaped the genetic distribution across the TMVB (Pérez-Crespo *et al.*, 2017; Mastretta-Yanes *et al.*, 2018; Bryson *et al.*, 2021; Cisneros-Bernal *et al.*, 2022), in some taxa promoting parapatric speciation processes (Ruiz-Sanchez & Specht, 2013; Mastretta-Yanes *et al.*, 2015; Baena-Díaz *et al.*, 2018). Other phylogeographical studies have documented genetic differentiation among populations of highland taxa distributed in the Mexican sierras (Sierra Madre Occidental, Sierra Madre Oriental, Sierra Madre del Sur and Sierra Madre de Chiapas), including those along the TMVB (e.g. Anducho-Reyes *et al.*, 2008; Bryson *et al.*, 2011a, b, c; McCormack *et al.*, 2011; Bryson & Riddle, 2012; Nolasco-Soto *et al.*, 2017; Venkatraman *et al.*, 2019; Anguiano-Constante *et al.*, 2021). In most studied cases, divergence events might have occurred during the Middle Miocene (from 5 to 3 Mya), coinciding with the genesis of the Sierra Madre Occidental and the western end of the TMVB (Zarza *et al.*, 2008; Suárez-Atilano *et al.*, 2014; Sánchez-González *et al.*, 2021) and splits in the eastern end of the TMVB during the Late Miocene, with a division of the Gulf Coastal Plain into north and south sides in the central area of the state of Veracruz (Zaldívar-Riverón *et al.*, 2004; Mulcahy *et al.*, 2006). However, the role of this geographical barrier, along with more recent Pleistocene climatic fluctuations restricting gene flow between populations north and south of the TMVB, has not been investigated to any large extent for lowland species. Previous studies in highland species implicate the TMVB as a porous barrier driving genetic divergence between populations north and south of the TMVB (Ornelas *et al.*, 2010; Ruiz-Sanchez & Ornelas, 2014; Rodríguez-Gómez & Ornelas, 2015, 2018; Anguiano-Constante *et al.*, 2021). Our study shows that the TMVB has been a geographical barrier to gene flow between northern and southern populations of the lowland hummingbird species *A. yucatanensis* and highlights the importance of the TMVB in driving isolation and genetic divergence between *A. yucatanensis* populations distributed north (CHA) and south (YUC+CER) of the volcanic belt.

The use of single-locus (mtDNA) sequence data in avian phylogeography has been questioned because it retrieves a biased species history owing to the stochastic nature of the coalescence process or effects of selection (e.g. Edwards & Beerli, 2000; Ballard & Whitlock, 2004; Edwards & Bensch, 2009). However, empirical evidence suggests that mtDNA is a powerful marker, more likely to detect population divergence than any other single locus owing to its smaller effective size, and thus faster coalescent time, to assess genetic variation between bird populations and to infer the underlying process affecting the geographical distribution of haplotypes (reviewed by Hung *et al.*, 2016). Thus, for more complex scenarios, such as multiple populations with mtDNA introgression, the existence of sex-biased dispersal and for estimation of both effective population size and intrapopulation genetic diversity, which is sensitive to changes in population size, multiple loci are required for accurate estimates (Piertney *et al.*, 2000; Zink & Barrowclough, 2008; Hung *et al.*, 2016).

Demographic history

In general, populations of Mesoamerican hummingbird species have shown contrasting responses to Pleistocene climate oscillations, including: (1) a lack of or weak signals of recent population expansion or changes in population size before the LGM (Jiménez & Ornelas, 2016; Ornelas *et al.*, 2016b; Zamudio-Beltrán & Hernández-Baños, 2018; Zamudio-Beltrán *et al.*, 2020b); or (2) demographic expansion and

increased population size after the LGM (Rodríguez-Gómez *et al.*, 2013) or between the LGM and the LIG (Rodríguez-Gómez & Ornelas, 2015; Hernández-Soto *et al.*, 2018). Here, the presence of many low-frequency single haplotypes separated by few mutational steps from high-frequency haplotypes within each haplogroup indicates rapid population growth from ancestral populations with small effective population size (Avise, 2000). Also, mismatch distributions, values of neutrality tests and BSPs suggest past demographic expansion without changes in the effective population size over time for *A. yucatanensis* genetic groups, particularly the CHA population (*A. y. chalconota*), which putatively expanded its range northwards in response to the Pleistocene glacial cycles. Although mismatch distributions and BSPs largely reflect demographic history, and the observed signatures of population expansion in *A. yucatanensis* populations appear to reflect responses to postglacial climate warming, cautions with sequence mismatch analysis and BSPs must be considered because several variables (e.g. sample size, levels of sequence polymorphism and estimates of mutation rates) might introduce errors in reconstructions of demographic history and the timing of population-level events (reviewed by Grant, 2015).

Morphometric analysis

Morphometric analysis showed significant variation among subspecies despite the large distributional range of *A. yucatanensis*. Overall, *A. y. yucatanensis* (YUC) individuals are smaller, and *A. y. chalconota* (CHA) individuals have significantly longer bills and are generally larger than YUC and *A. y. cerviniventris* (CER; Fig. 5). These results could be associated with changes in habitat, because the habitat of *A. y. chalconota* is significantly drier and warmer than the habitat occupied by the other subspecies (Vásquez-Aguilar *et al.*, 2021). Also, differences in body size between CHA and the other subspecies might be the result of geographical isolation independent of environmental pressure (Seeholzer & Brumfield, 2018), particularly for bill size, which might be more tightly constrained than body size owing to the feeding ecology of the species (Rodríguez-Gómez *et al.*, 2013; Rodríguez-Gómez & Ornelas, 2018; Vázquez-López *et al.*, 2021). Previous studies on hummingbird species have suggested that morphological differences between lineages are maintained by ecological adaptation (González *et al.*, 2011; Tovilla-Sierra *et al.*, 2019); that is, differences in environmental conditions provide the potential for ecological differentiation where differential selection pressures might act to shape the relationships between pollinator and plant species, causing differences in morphometric traits (González *et al.*, 2011; Rodríguez-Gómez *et al.*, 2013, 2021; Tovilla-Sierra *et al.*, 2019).

Palaeodistribution modelling and niche divergence

Projections on the distribution of suitable habitat in past conditions revealed that suitable habitat for *A. yucatanensis* was continuous along the Gulf of Mexico slope during the LIG but more restricted in the extreme north-east portion in comparison to its present distribution. During the LGM and MH to present conditions, the distribution of suitable habitat was overall more contracted and fragmented at the TMVB and more expanded on the Yucatán Peninsula and northwards to the USA. These results suggest that cyclical glacial expansions played a predominant role in the northward range expansion of CHA, and range contraction and fragmentation at the TMVB during these glacial periods could be responsible for the observed genetic differentiation by isolation. Our estimates of time since expansion suggest that *A. y. chalconota* and *A. y. cerviniventris* started before during the LIG (Table 2), whereas for *A. y. yucatanensis* the time since expansion was between the LGM and MH on the Yucatán Peninsula, which is currently covered by seasonally dry tropical deciduous forests (Licona-Vera *et al.*, 2018b).

Preglacial population expansion has been reported for some hummingbird species in the Mesoamerican region. The demographic expansion and range expansion of CHA into northern Tamaulipas and Texas generally concur with a northern range expansion in response to Pleistocene glacial–interglacial cycles in several hummingbird species, including *Leucolia* (= *Amazilia*) *violiceps* (Rodríguez-Gómez & Ornelas, 2015), *Colibri thalassinus* (Hernández-Soto *et al.*, 2018), *Eugenes fulgens* (Zamudio-Beltrán *et al.*, 2020b) and *Basilinna* (=*Hylocharis*) *leucotis* (Zamudio-Beltrán *et al.*, 2020a), and a northern range expansion and the evolution of long-distance seasonal migration linked with the LGM in *Selasphorus platycercus* (Malpica & Ornelas, 2014) and *Calothorax lucifer* (Licona-Vera *et al.*, 2018a). The expanded area of suitable habitat in more arid regions after the LGM suggests a strong adaptability of *A. y. chalconota*, currently isolated from the other subspecies, to varying conditions across its breeding range. This hypothesis is supported by ENMs under future climate change scenarios predicting a northward expansion in the distribution of *A. y. chalconota* into northern Texas and current northward expansion during the last 50 years in the USA, probably attributable to urbanization and supplementary feeding (Vásquez-Aguilar *et al.*, 2021; A.A. Vásquez-Aguilar, J.F. Ornelas, F. Rodríguez-Gómez & M.C. MacSwiney, unpublished data), which favour medium-sized hummingbirds with relatively long bills, as shown for hummingbird species in urban environments of central Mexico (Puga-Caballero *et al.*, 2020).

According to ENM, we showed that the distributions of suitable habitat for YUC and CER were connected

during the LIG, LGM and present conditions but fragmented during the MH (MIROC and CCSM), mainly in Tabasco (Figs 4, 5A). The recent fragmentation between YUC and CER populations during the MH according to the ENMs seems to explain their low genetic differentiation. Along with the demographic expansion and time since the demographic expansion, this suggests recent secondary contact between the ranges of YUC (*A. y. yucatanensis*) and CER (*A. y. cerviniventris*), which are currently connected, and that gene flow homogenized their genetic diversity accumulated by the effects of isolation during the MH. Further study using faster molecular markers (e.g. microsatellites) and additional sampling, particularly in Tabasco (Fig. 5), should provide finer resolution of genetic structure and detection of processes influenced by short periods of time.

The ENMs also indicated that the area of suitable habitat for *A. yucatanensis* was fragmented during the LGM, particularly at the TMVB. Following geographical isolation by the TMVB, it is possible that the divergence between CHA populations north of the TMVB and the other two genetic groups distributed south of the TMVB would have been reinforced by their differing environmental conditions. The result of genetic structuring and higher genetic differentiation between CHA and the other subspecies is consistent with the ENM results, suggesting low levels of dispersal and gene flow between populations separated by the TMVB. This scenario is also supported by niche overlap and niche equivalency tests, which indicated that the three mtDNA groups have similar but not equivalent niches and moderate to low niche overlap (Table 3). At the extremes of the species geographical distribution, subspecies *A. y. yucatanensis* (YUC) and *A. y. chalconota* (CHA) occupy considerably different environmental niches, whereas *A. y. cerviniventris* (CER) at the centre of the species distribution occupies an environmental niche relatively more related to the YUC niche than to the CHA niche (Table 3). This suggests great variability in their environmental space and suggests that the distribution of one subspecies cannot be implied by the distribution of another one (Vásquez-Aguilar *et al.*, 2021).

The three genetic groups of *A. yucatanensis* occupy similar environmental space (fundamental niche), probably owing to shared ancestral habitat preferences (niche conservatism; Wiens & Graham, 2005; Soberón & Nakamura, 2009). If allopatric fragmentation in *A. yucatanensis* occurred at the TMVB (and Tabasco; Fig. 5), one would expect genetically divergent groups of populations to retain certain aspects of their fundamental niche (E. González-Rodríguez, A.A. Vásquez-Aguilar & J.F. Ornelas, unpublished data). However, differences in niche equivalency (niches spaces are not interchangeable) suggest niche divergence between mtDNA groups (YUC, CER and CHA); although allopatric fragmentation might have been important for population differentiation of *A. y. chalconota* (CHA), abiotic factors driving niche divergence could not be ruled out as a contributor to its genetic differentiation.

The environmental niches of the three subspecies (mtDNA groups YUC, CER and CHA) are similar in terms of temperature and precipitation based on the PCA-env results, which are directly related to the availability of floral resources and thus the limiting factor in the distribution of genetic groups (Rodríguez-Gómez *et al.*, 2013; Abrahamczyk & Kessler 2015; Tovilla-Sierra *et al.*, 2019; E. González-Rodríguez, A.A. Vásquez-Aguilar & J.F. Ornelas, unpublished data). However, the environmental niches for the three genetic groups were not equivalent. For PC1 (60.5% of total variation), the PCA-env showed that the greater differences among subspecies correspond to differences in temperature and precipitation variables: PC1 is positively associated with the isothermality (BIO3), mean temperature of wettest quarter (BIO4), temperature annual range (BIO7) and precipitation of wettest month (BIO13) and negatively associated with precipitation seasonality (BIO15) and precipitation of the driest quarter (BIO17). These results indicate that precipitation variables might be more important than temperature in determining the limits in the distribution of all three mtDNA genetic groups. Thus, our findings based on the non-equivalency of the fundamental niches support the hypothesis that the mtDNA genetic groups of *A. yucatanensis* have undergone coarse-scale niche divergence and are constrained by a set of climatic and macro-environmental conditions that might determine the distribution and availability of floral resources that *A. yucatanensis* interacts with within each of the regions, as observed for the sister species *Amazilia rutila* inhabiting seasonally dry tropical deciduous forest on the Pacific slope of Mexico and the Yucatán Peninsula (E. González-Rodríguez, A.A. Vásquez-Aguilar & J.F. Ornelas, unpublished data).

Conclusions

The use of integrative phylogeography is basic to determining which taxonomic unit is important to species conservation. By reconstructing the phylogeography and distribution of suitable habitat through coupling genetic, morphometric and ecological data with past ecological niche models and niche divergence tests, we have highlighted genetic (mtDNA) and morphological differentiation among populations of *A. yucatanensis* subspecies. Although we showed evidence of two mtDNA genetic groups and demographic population expansion was detected,

further sampling and more variable nuclear markers are required to make inferences about the demographic consequences of isolation and subspecies recognition.

ACKNOWLEDGEMENTS

We are grateful to Cristina Bárcenas, Yuyini Licona-Vera, Mariana Hernández-Soto, Diego F. Angulo, Ernesto A. López-Huicochea, Evelyn González-Rodríguez, José Manuel García-Enríquez, Juan Cruzado Cortés and Jorge Antonio Gómez Díaz for field and laboratory assistance and data analysis; Patricia Escalante and Marco A. Gurrola (Colección Nacional de Aves, IBUNAM) and Fanny Rebón (MZFC) for allowing us to take morphological measurements on museum specimens; and Professor John A. Allen and two anonymous for providing useful comments on the manuscript. The collection of samples in Mexico was conducted with the permission of the Secretaría de Medio Ambiente y Recursos Naturales, Instituto de Ecología, Dirección General de Vida Silvestre (permit numbers: INE SEMARNAP, D00-02/3269, INE SGPA/DGVS/02038/07, 01568/08, 02517/09, 07701/11, 13528/14, 02577/15, 06448/16 and 5050/19). This research was funded by research competitive grants (grant numbers 61710, 155686 and A1-S-26134) from the Consejo Nacional de Ciencia y Tecnología (CONACyT; https://www.conacyt.mx) and research funds (20030/10563) from the Departamento de Biología Evolutiva, Instituto de Ecología, A.C. (INECOL; https://www.inecol.mx/inecol/index.php/es/ct-menu-item-1/redes-tematicas/biologia-evolutiva) to J.F.O. and the Centro de Investigaciones Tropicales (CITRO), Universidad Veracruzana. The authors have no conflicts of interest to declare. This work constitutes partial fulfilment of A.A.V-A.'s doctorate in the Tropical Ecology programme at the Centro de Investigaciones Tropicales (CITRO), Universidad Veracruzana.

DATA AVAILABILITY

All unique sequences used in this study have been deposited in GenBank under the following accession numbers: *ND2* locus, OP946811–OP946874; *ATPase* 6 and 8, OP946747–OP946810.

REFERENCES

Abrahamczyk S, **Kessler M. 2015**. Morphological and behavioural adaptations to feed on nectar: how feeding ecology determines the diversity and composition of hummingbird assemblages. *Journal of Ornithology* **156**: 333–347.

Anducho-Reyes MA, **Cognato AI**, **Hayes JL**, **Zúñiga G. 2008**. Phylogeography of the bark beetle *Dendroctonus mexicanus* Hopkins (Coleoptera: Curculionidae: Scolytinae). *Molecular Phylogenetics and Evolution* **49**: 930–940.

Anguiano-Constante MA, **Zamora-Tavares P**, **Ruiz-Sánchez E**, **Dean E**, **Rodríguez A**, **Munguía-Lino G. 2021**. Population differentiation and phylogeography in *Lycianthes moziniana* (Solanaceae: Capsiceae), a perennial herb endemic to the Mexican Transition Zone. *Biological Journal of the Linnean Society* **132**: 359–373.

Atauchi PJ, **Aucca-Chutas C**, **Ferro G**, **Prieto-Torres DA. 2020**. Present and future potential distribution of the endangered *Anairetes alpinus* (Passeriformes: Tyrannidae) under global climate change scenarios. *Journal of Ornithology* **161**: 723–738.

Avise JC. 2000. *Phylogeography: the history and formation of species*. Cambridge: Harvard University Press.

Baena-Díaz F, **Ramírez-Barahona S**, **Ornelas JF. 2018**. Hybridization and differential introgression associated with environmental shifts in a mistletoe species complex. *Scientific Reports* **8**: 5591.

Ballard JWO, **Whitlock MC. 2004**. The incomplete natural history of mitochondria. *Molecular Ecology* **13**: 729–744.

Bandelt HJ, **Forster P**, **Rohl A. 1999**. Median-joining networks for inferring intraspecific phylogenies. *Molecular Biology and Evolution* **16**: 37–48.

Barve N, **Barve V**, **Jiménez-Valverde A**, **Lira-Noriega A**, **Maher SP**, **Peterson AT**, **Soberón J**, **Villalobos F. 2011**. The crucial role of the accessible area in ecological niche modeling and species distribution modeling. *Ecological Modelling* **222**: 1810–1819.

Bent AC. 1940. Life histories of North American cuckoos, goatsuckers, hummingbirds, and their allies. *United States National Museum Bulletin* **176**: 1–506.

Booth TH, **Nix HA**, **Busby JR**, **Hutchinson MF. 2014**. BIOCLIM: the first species distribution modelling package, its early applications and relevance to most current MAXENT studies. *Diversity and Distributions* **20**: 1–9.

Borzée A, **Andersen D**, **Groffen J**, **Kim HT**, **Bae Y**, **Jang Y. 2019**. Climate change-based models predict range shifts in the distribution of the only Asian plethodontid salamander: *Karsenia koreana*. *Scientific Reports* **9**: 11838.

Bouckaert R, **Heled J**, **Kühnert D**, **Vaughan T**, **Wu C-H**, **Xie D**, **Suchard MA**, **Rambaut A**, **Drummond AJ. 2014**. BEAST 2: a software platform for Bayesian evolutionary analysis. *PLoS Computational Biology* **10**: e1003537.

Braconnot P, **Otto-Bliesner B**, **Harrison S**, **Joussaume S**, **Peterschmitt J-Y**, **Abe-Ouchi A**, **Crucifix M**, **Driesschaert E**, **Fichefet T**, **Hewitt CD**, **Kageyama M**, **Kitoh A**, **Loutre M-F**, **Marti O**, **Merkel U**, **Ramstein G**, **Valdes P**, **Weber L**, **Yu Y**, **Zhao Y. 2007**. Results of PMIP2 coupled simulations of the Mid-Holocene and Last Glacial Maximum – Part 2: feedbacks with emphasis on the location of the ITCZ and mid- and high latitudes heat budget. *Climate Past* **3**: 279–296.

Broennimann O, **Fitzpatrick MC**, **Pearman PB**, **Petitpierre B**, **Pellissier L**, **Yoccoz NG**, **Thuiller W**, **Fortin MJ**, **Randin C**, **Zimmermann NE**, **Graham CH**, **Guisan A. 2012**. Measuring ecological niche overlap from occurrence and spatial environmental data. *Global Ecology and Biogeography* **21**: 481–497.

Brush JS, **Brush T**, **Racelis A. 2020**. Effects of urbanization on Buff-bellied Hummingbirds in subtropical South Texas. *Cities and the Environment* **13**: 1.

Bryson RW Jr, **García-Vázquez UO**, **Riddle BR. 2011a**. Phylogeography of Middle American gophersnakes: mixed responses to biogeographical barriers across the Mexican Transition Zone. *Journal of Biogeography* **38**: 1570–1584.

Bryson RW Jr, **Grummer JA**, **Connors EM**, **Tirpak J**, **McCormack JE**, **Klicka J. 2021**. Cryptic diversity across the Trans-Mexican Volcanic Belt of Mexico in the montane bunchgrass lizard *Sceloporus subniger* (Squamata: Phrynosomatidae). *Zootaxa* **4963**: 335–353.

Bryson RW Jr, **Murphy RW**, **Graham MR**, **Lathrop A**, **Lazcano-Villareal D. 2011b**. Ephemeral Pleistocene woodlands connect the dots for highland rattlesnakes of the *Crotalus intermedius* group. *Journal of Biogeography* **38**: 2299–2310.

Bryson RW Jr, **Murphy RW**, **Lathrop A**, **Lazcano-Villareal D. 2011c**. Evolutionary drivers of phylogeographical diversity in the highlands of Mexico: a case study of the *Crotalus triseriatus* species group of montane rattlesnakes. *Journal of Biogeography* **38**: 697–710.

Bryson RW Jr, **Riddle BR. 2012**. Tracing the origins of widespread highland species: a case of Neogene diversification across the Mexican sierras in an endemic lizard. *Biological Journal of the Linnean Society* **105**: 382–394.

Cavers S, **Navarro C**, **Lowe AJ. 2003**. Chloroplast DNA phylogeography reveals colonization history of a Neotropical tree, *Cedrela odorata* L., in Mesoamerica. *Molecular Ecology* **12**: 1451–1460.

Chávez-Ramírez F, **Moreno-Valdéz A. 2020**. Buff-bellied hummingbird (*Amazilia yucatanensis*), version 1.0. In: Poole AF, ed. *Birds of the World*. Ithaca: Cornell Lab of Ornithology.

Cisneros-Bernal AY, **Rodríguez-Gómez F**, **Flores-Villela O**, **Fujita MK**, **Velasco JA**, **Fernández JA. 2022**. Phylogeography supports lineage divergence for an endemic rattlesnake (*Crotalus ravus*) of the Neotropical montane forest in the Trans-Mexican Volcanic Belt. *Biological Journal of the Linnean Society* **137**: 496–512.

Clement M, **Posada D**, **Crandall KA. 2000**. TCS: a computer program to estimate genealogies. *Molecular Ecology* **9**: 1657–1659.

Cobos ME, **Peterson AT**, **Barve N**, **Osorio-Olvera L. 2019**. kuenm: an R package for detailed development of ecological niche models using Maxent. *PeerJ* **7**: e6281.

Collins WD, **Blackmon M**, **Bitz C**, **Bonan G**, **Bretherton CS. 2004**. The community climate system model: CCSM3. *Journal of Climate* **19**: 2122–2143.

Corander J, **Sirén J**, **Arjas E. 2008**. Bayesian spatial modeling of genetic population structure. *Computer Statistics* **23**: 111–129.

Cortés-Rodríguez N, **Hernández-Baños BE**, **Navarro-Sigüenza AG**, **Peterson AT**, **García-Moreno J. 2008**. Phylogeography and population genetics of the Amethyst-throated Hummingbird (*Lampornis amethystinus*). *Molecular Phylogenetics and Evolution* **48**: 1–11.

Darriba D, **Taboada GL**, **Doallo R**, **Posada D. 2012**. jModelTest 2: more models, new heuristics and parallel computing. *Nature Methods* **9**: 772.

Dickinson EC, **Remsen JV. 2013**. *The Howard and Moore complete checklist of the birds of the world, Vol. 1, Non-passerines*. Eastbourne: Aves Press.

Di Cola V, **Broennimann O**, **Petitpierre B**, **Breiner FT**, **D'Amen M**, **Randin C**, **Engler R**, **Pottier J**, **Pio D**, **Dubuis A**, **Pellissier L**, **Mateo RG**, **Hordijk W**, **Salamin N**, **Guisan A. 2017**. ecospat: an R package to support spatial analyses and modeling of species niches and distributions. *Ecography* **40**: 774–787.

Dormann CF, **Elith J**, **Bacher S**, **Buchmann C**, **Carl G**, **Carré G**, **García-Marquéz JR**, **Gruber B**, **Lafourcade B**, **Leitao PJ**, **Münkemüller T**, **McClean C**, **Osborne PE**, **Reineking B**, **Schroder B**, **Skidmore A**, **Zurell D**, **Lautenbach S. 2013**. Collinearity: a review of methods to deal with it and a simulation study evaluating their performance. *Ecography* **36**: 27–46.

Drummond AJ, **Rambaut A. 2007**. BEAST: Bayesian evolutionary analysis by sampling trees. *BMC Evolutionary Biology* **7**: 214.

Drummond AJ, **Rambaut A**, **Shapiro B**, **Pybus OG. 2005**. Bayesian coalescent inference of past population dynamics from molecular sequences. *Molecular Biology and Evolution* **22**: 1185–1192.

Dupanloup I, **Schneider S**, **Excoffier L. 2002**. A simulated annealing approach to define the genetic structure of populations. *Molecular Ecology* **11**: 2571–2581.

Eberhard JR, **Bermingham E**, **Zink R. 2004**. Phylogeny and biogeography of the *Amazona ochrocephala* (Aves: Psittacidae) complex. *The Auk* **121**: 318–332.

Edwards SV, **Beerli P. 2000**. Perspective: gene divergence, population divergence, and the variance in coalescence time in phylogeographic studies. *Evolution* **54**: 1839–1854.

Edwards S, **Bensch S. 2009**. Looking forwards or looking backwards in avian phylogeography? A comment on Zink and Barrowclough 2008. *Molecular Ecology* **18**: 2930–2933; discussion 2934.

Elith J, **Phillips SJ**, **Hastie T**, **Dudík M**, **Chee YE**, **Yates CJ. 2011**. A statistical explanation of MaxEnt for ecologists. *Diversity and Distributions* **17**: 43–57.

ESRI. **2016**. *ArcGis Desktop 10.5*. Redlands: Environmental System Research Institute.

Excoffier L. 2004. Patterns of DNA sequence diversity and genetic structure after a range expansion: lessons from the infinite-island model. *Molecular Ecology* **13**: 853–864.

Excoffier L, **Lischer HEL. 2010**. Arlequin suite ver 3.5: a new series of programs to perform population genetics analyses under Linux and Windows. *Molecular Ecology Resources* **10**: 564–567.

Excoffier L, **Smouse PE**, **Quattro JM. 1992**. Analysis of molecular variance inferred from metric distances among DNA haplotypes: Application to human mitochondrial DNA restriction data. *Genetics* **131**: 479–491.

Freeman B, **Sunnarborg J**, **Peterson AT. 2019**. Effects of climate change on the distributional potential of three range-restricted West African bird species. *The Condor* **121**: duz012.

Friedmann H, **Griscom L**, **Moore RT. 1950**. Distributional check-list of the birds of Mexico. Part 1. *Pacific Coast Avifauna* **29**: 1–202.

Fu Y. 1997. Statistical neutrality of mutations against population growth, hitchhiking and background selection. *Genetics* **147**: 915–925.

González C, **Ornelas JF**, **Gutiérrez-Rodríguez C. 2011**. Selection and geographic isolation influence hummingbird

speciation: genetic, acoustic and morphological divergence in the wedge-tailed sabrewing (*Campylopterus curvipennis*). *BMC Evolutionary Biology* **11**: 38.

González-Rubio C, **Garcia-De Leon FJ**, **Rodriguez-Estrella R. 2016**. Phylogeography of endemic Xantus' hummingbird (*Hylocharis xantusii*) shows a different history of vicariance in the Baja California Peninsula. *Molecular Phylogenetics and Evolution* **102**: 265–277.

Grant WS. 2015. Problems and cautions with sequence mismatch analysis and Bayesian skyline plots to infer historical demography. *Journal of Heredity* **106**: 333–346.

Gutiérrez-García TA, **Vázquez-Domínguez E. 2012**. Biogeographically dynamic genetic structure bridging two continents in the monotypic Central American rodent *Ototylomys phyllotis*. *Biological Journal of the Linnean Society* **107**: 593–610.

Gutiérrez-Rodríguez C, **Ornelas JF**, **Rodríguez-Gómez F. 2011**. Chloroplast DNA phylogeography of a distylous shrub (*Palicourea padifolia*, Rubiaceae) reveals past fragmentation and demographic expansion in Mexican cloud forests. *Molecular Phylogenetics and Evolution* **61**: 603–615.

Hackett SJ. 1996. Molecular phylogenetics and biogeography of tanagers in the genus *Ramphocelus* (Aves). *Molecular Phylogenetics and Evolution* **5**: 368–382.

Hammer O, **Harper DA**, **Ryan PD. 2001**. PAST: paleontological statistics software package for education and data analysis. *Palaeontologia Electronica* **4**: 4.

Harpending RC. 1994. Signature of ancient population growth in a low-resolution mitochondrial DNA mismatch distribution. *Human Biology* **66**: 591–600.

Harvey MG, **Bonter DN**, **Stenzler LM**, **Lovette IJ. 2006**. A comparison of plucked feathers versus blood samples as DNA sources for molecular sexing. *Journal of Field Ornithology* **77**: 136–140.

Hasumi H, **Emori D. 2004**. *K-1 coupled GCM (MIROC) description*. Tokyo: Center for Climate System Research, University of Tokyo.

Hernández-Soto M, **Licona-Vera Y**, **Lara C**, **Ornelas JF. 2018**. Molecular and climate data reveal expansion and genetic differentiation of Mexican Violet-ear *Colibri thalassinus thalassinus* (Aves: Trochilidae) populations separated by the Isthmus of Tehuantepec. *Journal of Ornithology* **159**: 687–702.

Hijmans RJ, **Cameron SE**, **Parra JL**, **Jones PG**, **Jarvis A. 2005**. Very high resolution interpolated climate surfaces for global land areas. *International Journal of Climatology* **25**: 1965–1978.

Ho SY, **Shapiro B. 2011**. Skyline-plot methods for estimating demographic history from nucleotide sequences. *Molecular Ecology Resources* **11**: 423–434.

Howell SNG, **Webb S. 1995**. *A guide to the birds of Mexico and northern Central America*. New York: Oxford University Press.

Hung CM, **Drovetski SV**, **Zink RM. 2016**. Matching loci surveyed to questions asked in phylogeography. *Proceedings of the Royal Society B: Biological Sciences* **283**: 20152340.

Jiménez RA, **Ornelas JF. 2016**. Historical and current introgression in a Mesoamerican hummingbird species complex: a biogeographic perspective. *PeerJ* **4**: e1556.

Johnsgard PA. 1983. *The hummingbirds of North America*. Washington: Smithsonian Institution Press.

Kingston SE, **Navarro-Sigüenza AG**, **García-Trejo EA**, **Vázquez-Miranda H**, **Fagan WF**, **Braun MJ. 2014**. Genetic differentiation and habitat connectivity across towhee hybrid zones in Mexico. *Evolutionary Ecology* **28**: 277–297.

Lande R, **Engen S**, **Sæther BE. 2003**. *Stochastic population dynamics in ecology and conservation*. Oxford: Oxford University Press.

Leigh JW, **Bryant D. 2015**. Popart: full-feature software for haplotype network construction. *Methods in Ecology and Evolution* **6**: 1110–1116.

Lerner HRL, **Meyer M**, **James HF**, **Hofreiter M**, **Fleischer RC. 2011**. Multilocus resolution of phylogeny and timescale in the extant adaptive radiation of Hawaiian honeycreepers. *Current Biology* **21**: 1838–1844.

Licona-Vera Y, **Ornelas JF. 2014**. Genetic, ecological and morphological divergence between populations of the endangered Mexican Sheartail Hummingbird (*Doricha eliza*). *PLoS One* **9**: e101870.

Licona-Vera Y, **Ornelas JF**, **Wethington S**, **Bryan KB. 2018a**. Pleistocene range expansions promote divergence with gene flow between migratory and sedentary populations of *Calothorax* hummingbirds. *Biological Journal of the Linnean Society* **124**: 645–667.

Licona-Vera Y, **Ortiz-Rodriguez AE**, **Vásquez-Aguilar AA**, **Ornelas JF. 2018b**. Lay mistletoes on the Yucatán Peninsula: post-glacial expansion and genetic differentiation of *Psittacanthus mayanus* (Loranthaceae). *Botanical Journal of the Linnean Society* **186**: 334–360.

Lobo JM, **Jiménez-Valverde A**, **Real R. 2008**. AUC: a misleading measure of the performance of predictive distribution models. *Global Ecology and Biogeography* **17**: 145–151.

Maldonado-Sánchez D, **Gutiérrez-Rodríguez C**, **Ornelas JF. 2016**. Genetic divergence in the common bush-tanager *Chlorospingus ophthalmicus* (Aves: Emberizidae) throughout Mexican cloud forests: the role of geography, ecology and Pleistocene climatic fluctuations. *Molecular Phylogenetics and Evolution* **99**: 76–88.

Malpica A, **Ornelas JF. 2014**. Postglacial northward expansion and genetic differentiation between migratory and sedentary populations of the broad-tailed hummingbird (*Selasphorus platycercus*). *Molecular Ecology* **23**: 435–452.

Mastretta-Yanes A, **Moreno-Letelier A**, **Piñero D**, **Jorgensen TH**, **Emerson BC. 2015**. Biodiversity in the Mexican highlands and the interaction of geology, geography and climate within the Trans-Mexican Volcanic Belt. *Journal of Biogeography* **42**: 1586–1600.

Mastretta-Yanes A, **Xue AT**, **Moreno-Letelier A**, **Jorgensen TH**, **Alvarez N**, **Piñero D**, **Emerson BC. 2018**. Long-term in situ persistence of biodiversity in tropical sky islands revealed by landscape genomics. *Molecular Ecology* **27**: 432–448.

McCormack JE, **Heled J**, **Delaney KS**, **Peterson AT**, **Knowles LL. 2011**. Calibrating divergence times on species versus gene trees: implications for speciation history of *Aphelocoma* jays. *Evolution* **65**: 184–202.

Merow C, **Smith MJ**, **Edwards TC**, **Guisan A**, **McMahon SM**, **Normand S**, **Thuiller W**, **Wüest RO**, **Zimmermann NE**, **Elith J. 2014**. What do we gain from simplicity versus complexity in species distribution models? *Ecography* **37**: 1267–1281.

Miller MJ, **Lelevier MJ**, **Bermingham E**, **Klicka JT**, **Escalante P**, **Winker K. 2011**. Phylogeography of the Rufous-tailed Hummingbird (*Amazilia tzacatl*). *The Condor* **113**: 806–816.

Mulcahy DG, **Morrill BH**, **Mendelson IJ. 2006**. Historical biogeography of lowland species of toads (*Bufo*) across the Trans-Mexican Neovolcanic Belt and the Isthmus of Tehuantepec. *Journal of Biogeography* **33**: 1889–1904.

Müller K, **Müller J**, **Neinhuis C**, **Quandt D. 2006**. *PhyDE–phylogenetic data editor, v0.995*. Program distributed by the authors.

Nolasco-Soto J, **González-Astorga J**, **Espinosa de los Monteros A**, **Galante-Patiño E**, **Favila ME. 2017**. Phylogeographic structure of *Canthon cyanellus* (Coleoptera: Scarabaeidae), a Neotropical dung beetle in the Mexican Transition Zone: insights on its origin and the impacts of Pleistocene climatic fluctuations on population dynamics. *Molecular Phylogenetics and Evolution* **109**: 180–190.

Olson DM, **Dinerstein E**, **Wikramanayake ED**, **Burgess ND**, **Powell GVN**, **Underwood EC**, **D'amico JA**, **Itoua I**, **Strand HE**, **Morrison JC**, **Loucks CJ**, **Allnutt TF**, **Ricketts TH**, **Kura Y**, **Lamoreux JF**, **Wettengel WW**, **Hedao P**, **Kassem KR. 2001**. Terrestrial ecoregions of the world: a new map of life on Earth: A new global map of terrestrial ecoregions provides an innovative tool for conserving biodiversity. *BioScience* **51**: 933–938.

Ornelas JF, **Gándara E**, **Vásquez-Aguilar AA**, **Ramírez-Barahona S**, **Ortiz-Rodriguez AE**, **González C**, **Mejía Saules MT**, **Ruiz-Sanchez E. 2016a**. A mistletoe tale: postglacial invasion of *Psittacanthus schiedeanus* (Loranthaceae) to Mesoamerican cloud forests revealed by molecular data and species distribution modeling. *BMC Evolutionary Biology* **16**: 78.

Ornelas JF, **González C. 2014**. Interglacial genetic diversification of *Moussonia deppeana* (Gesneriaceae), a hummingbird-pollinated, cloud forest shrub in northern Mesoamerica. *Molecular Ecology* **23**: 4119–4136.

Ornelas JF, **González C**, **Hernández-Baños BE**, **García-Moreno J. 2016b**. Molecular and iridescent feather reflectance data reveal recent genetic diversification and phenotypic differentiation in a cloud forest hummingbird. *Ecology and Evolution* **6**: 1104–1127.

Ornelas JF, **González de León S**, **González C**, **Licona-Vera Y**, **Ortiz-Rodríguez AE**, **Rodríguez-Gómez F. 2015**. Comparative palaeodistribution of eight hummingbird species reveal a link between genetic diversity and habitat suitability and Quaternary climate-change stability in Mexico. *Folia Zoologica* **64**: 245–258.

Ornelas JF, **Rodríguez-Gómez F. 2015**. Influence of Pleistocene glacial/interglacial cycles on the genetic structure of the mistletoe cactus *Rhipsalis baccifera* (Cactaceae) in Mesoamerica. *Journal of Heredity* **106**: 196–210.

Ornelas JF, **Ruiz-Sanchez E**, **Sosa V. 2010**. Phylogeography of *Podocarpus matudae* (Podocarpaceae): pre-Quaternary relicts in northern Mesoamerican cloud forests. *Journal of Biogeography* **37**: 2384–2396.

Ornelas JF, **Sosa V**, **Soltis DE**, **Daza JM**, **González C**, **Soltis PS**, **Gutiérrez-Rodríguez C**, **Espinosa de los Monteros A**, **Castoe TA**, **Bell C**, **Ruiz-Sánchez E. 2013**. Comparative phylogeography analyses illustrate the complex evolutionary history of threatened cloud forests in northern Mesoamerica. *PLoS One* **8**: e56283.

Ortiz-Rodríguez AE, **Licona-Vera Y**, **Vásquez-Aguilar AA**, **Hernández-Soto M**, **López-Huicochea EA**, **Ornelas JF. 2020**. Genetic differentiation among *Psittacanthus rhynchanthus* (Loranthaceae) populations: novel phylogeographic patterns in the Mesoamerican tropical lowlands. *Plant Systematics and Evolution* **306**: 10.

Osorio-Olvera L, **Lira-Noriega A**, **Soberon J**, **Peterson AT**, **Falconi M**, **Contreras-Díaz RG**, **Martínez-Meyer E**, **Barve V**, **Barve N. 2020**. NTBOX: an R package with graphical user interface for modelling and evaluating multidimensional ecological niches. *Methods in Ecology and Evolution* **11**: 1199–1206.

Otto-Bliesner BL, **Hewitt CD**, **Marchitto TM**, **Brady E**, **Abe-Ouchi A**, **Crucifix M**, **Murakami S**, **Weber SL. 2007**. Last Glacial Maximum ocean thermohaline circulation: PMIP2 model intercomparisons and data constraints. *Geophysical Research Letters* **34**: L12706.

Otto-Bliesner BL, **Marshall SJ**, **Overpeck JT**, **Miller GH**, **Hu A. 2006**. Simulating arctic climate warmth and icefield retreat in the Last Interglaciation. *Science* **311**: 1751–1753.

Owens HL, **Campbell LP**, **Dornak LL**, **Saupe EE**, **Barve N**, **Soberón J**, **Ingenloff K**, **Lira-Noriega A**, **Hensz CM**, **Myers CE**, **Peterson TA. 2013**. Constraints on interpretation of ecological niche models by limited environmental ranges on calibration areas. *Ecological Modelling* **263**: 10–18.

Papadopoulou A, **Knowles LL. 2016**. Toward a paradigm shift in comparative phylogeography driven by trait-based hypotheses. *Proceedings of the National Academy of Sciences of the United States of America* **113**: 8018–8024.

Paradis E. 2010. pegas: an R package for population genetics with an integrated–modular approach. *Bioinformatics* **26**: 419–420.

Parra-Olea G, **Windfield JC**, **Velo-Anton G**, **Zamudio KR. 2012**. Isolation in habitat refugia promotes rapid diversification in a montane tropical salamander. *Journal of Biogeography* **39**: 353–370.

Pearson RG, **Raxworthy CJ**, **Nakamura M**, **Peterson AT. 2007**. Predicting species distributions from small numbers of occurrence records: a test case using cryptic geckos in Madagascar. *Journal of Biogeography* **34**: 102–117.

Pérez-Crespo MJ, **Ornelas JF**, **González-Rodríguez A**, **Ruiz-Sanchez E**, **Vásquez-Aguilar AA**, **Ramírez-Barahona S. 2017**. Phylogeography and population differentiation in the *Psittacanthus calyculatus* (Loranthaceae) mistletoe: a complex scenario of climate–volcanism interaction along the Trans-Mexican Volcanic Belt. *Journal of Biogeography* **44**: 2501–2514.

Peterson AT, **Papeş M**, **Soberón J. 2008**. Rethinking receiver operating characteristic analysis applications in ecological niche modeling. *Ecological Modelling* **213**: 63–72.

Pfenninger M, **Posada D. 2002**. Phylogeographic history of the land snail *Candidula unifasciata* (Helicellinae, Stylommatophora): fragmentation, corridor migration, and secondary contact. *Evolution* **56**: 1776–1788.

Phillips SJ, **Anderson RP**, **Dudík M**, **Schapire RE**, **Blair ME. 2017**. Opening the black box: an open-source release of Maxent. *Ecography* **40**: 887–893.

Phillips SJ, **Anderson RP**, **Schapire RE. 2006**. Maximum entropy modeling of species geographic distributions. *Ecological Modelling* **190**: 231–259.

Piertney SB, **MacColl ADC**, **Bacon PJ**, **Racey PA**, **Lambin X**, **Dallas JF. 2000**. Matrilineal genetic structure and female-mediated gene flow in red grouse (*Lagopus lagopus scoticus*): an analysis using mitochondrial DNA. *Evolution* **54**: 279–289.

Pons O, **Petit RJ. 1996**. Measuring and testing genetic differentiation with ordered versus unordered alleles. *Genetics* **144**: 1237–1245.

Prieto-Torres DA, **Lira-Noriega A**, **Navarro-Sigüenza AG. 2020**. Climate change promotes species loss and uneven modification of richness patterns in the avifauna associated to Neotropical seasonally dry forests. *Perspectives in Ecology and Conservation* **18**: 19–30.

Puga-Caballero A, **Arizmendi MC**, **Sánchez-González LA. 2020**. Phylogenetic and phenotypic filtering in hummingbirds from urban environments in Central Mexico. *Evolutionary Ecology* **34**: 525–241.

R Development Core Team. 2020. *R: a language and environment for statistical computing*. Vienna: R Foundation for Statistical Computing.

Rambaut A, **Drummond AJ**, **Xie D**, **Baele G**, **Suchard MA. 2018**. Posterior summarization in Bayesian phylogenetics using Tracer 1.7. *Systematic Biology* **67**: 901–904.

Ramírez-Barahona S, **Eguiarte LE. 2014**. Changes in the distribution of cloud forests during the last glacial predict the patterns of genetic diversity and demographic history of the tree fern *Alsophila firma* (Cyatheaceae). *Journal of Biogeography* **41**: 2396–2407.

Ramos-Onsins R, **Rozas R. 2002**. Statistical properties of new neutrality tests against population growth. *Molecular Biology and Evolution* **19**: 2092–2100.

Rodríguez-Gómez F, **Gutiérrez-Rodríguez C**, **Ornelas JF. 2013**. Genetic, phenotypic and ecological divergence with gene flow at the Isthmus of Tehuantepec: the case of the azure-crowned hummingbird (*Amazilia cyanocephala*). *Journal of Biogeography* **40**: 1360–1373.

Rodríguez-Gómez F, **Licona-Vera Y**, **Silva-Cárdenas L**, **Ornelas JF. 2021**. Phylogeography, morphology and ecological niche modelling to explore the evolutionary history of Azure-crowned Hummingbird (*Amazilia cyanocephala*, Trochilidae) in Mesoamerica. *Journal of Ornithology* **162**: 529–547.

Rodríguez-Gómez F, **Ornelas JF. 2014**. Genetic divergence of the Mesoamerican azure-crowned hummingbird (*Amazilia cyanocephala*, Trochilidae) across the Motagua-Polochic-Jocotán fault system. *Journal of Zoological Systematics and Evolutionary Research* **52**: 142–153.

Rodríguez-Gómez F, **Ornelas JF. 2015**. At the passing gate: past introgression in the process of species formation between *Amazilia violiceps* and *A. viridifrons* hummingbirds along the Mexican Transition Zone. *Journal of Biogeography* **42**: 1305–1318.

Rodríguez-Gómez F, **Ornelas JF. 2018**. Genetic structuring and secondary contact in the white-chested *Amazilia* hummingbird species complex. *Journal of Avian Biology* **49**: jave01536.

Rogers AR, **Harpending H. 1992**. Population growth makes waves in the distribution of pairwise genetic differences. *Molecular Biology and Evolution* **9**: 552–569.

Ruiz-Gutiérrez V, **Doherty PF**, **Santana E**, **Contreras Martínez S**, **Schondube J**, **Verdugo Munguía H**, **Iñigo-Elias E. 2012**. Survival of resident Neotropical birds: considerations for sampling and analysis based on 20 years of bird-banding efforts in Mexico. *The Auk* **129**: 500–509.

Ruiz-Sanchez E, **Ornelas JF. 2014**. Phylogeography of *Liquidambar styraciflua* (Altingiaceae) in Mesoamerica: survivors of a Neogene widespread temperate forest (or cloud forest) in North America? *Ecology and Evolution* **4**: 311–328.

Ruiz-Sanchez E, **Specht CD. 2013**. Influence of the geological history of the Trans-Mexican Volcanic Belt on the diversification of *Nolina parviflora* (Asparagaceae: Nolinoideae). *Journal of Biogeography* **40**: 1336–1347.

Ruiz-Sanchez E, **Specht CD. 2014**. Ecological speciation in *Nolina parviflora* (Asparagaceae): lacking spatial connectivity along the Trans-Mexican Volcanic Belt. *PLoS One* **9**: e98754.

Russell RW, **Carpenter FL**, **Hixon MA**, **Paton DC. 1994**. The impact of variation in stopover habitat quality on migrant rufous hummingbirds. *Conservation Biology* **8**: 483–490.

Sánchez-González LA, **Castillo-Chora VJ**, **Arbeláez-Cortés E**, **Navarro-Sigüenza AG. 2021**. Diversification and secondary contact in the magpie-jays (*Calocitta*) throughout the pacific lowlands of Mesoamerica. *Journal of Zoological Systematics and Evolutionary Research* **59**: 2371–2386.

Schneider S, **Excoffier L. 1999**. Estimation of past demographic parameters from the distribution of pairwise differences when the mutation rates vary among sites: application to human mitochondrial DNA. *Genetics* **152**: 1079–1089.

Schoener TW. 1970. Nonsynchronous spatial overlap of lizards in patchy habitats. *Ecology* **51**: 408–418.

Schuchmann K-L. 1999. Family Trochilidae, hummingbirds. In del Hoyo J, Elliott A, Sargatal J, eds. *Handbook of the birds of the world, Vol. 5*. Barcelona: Lynx Edicions, 468–680.

Seeholzer GF, **Brumfield RT. 2018**. Isolation by distance, not incipient ecological speciation, explains genetic differentiation in an Andean songbird (Aves: Furnariidae: *Cranioleuca antisiensis*, Line-cheeked Spinetail) despite near threefold body size change across an environmental gradient. *Molecular Ecology* **27**: 279–296.

Soberón J, **Nakamura M. 2009**. Niches and distributional areas: concepts, methods, and assumptions. *Proceedings of the National Academy of Sciences of the United States of America* **106**: 19644–19650.

Soberón J, **Peterson AT. 2005**. Interpretation of models of fundamental ecological niches and species' distributional areas. *Biodiversity Informatics* **2**: 1–10.

Sorenson MD, **Ast JC**, **Dimcheff DE**, **Yuri T**, **Mindell DP. 1999**. Primers for a PCR-based approach to mitochondrial genome sequencing in birds and other vertebrates. *Molecular Phylogenetics and Evolution* **12**: 105–114.

Strubbe D, **Beauchard O**, **Matthysen E. 2015**. Niche conservatism among non-native vertebrates in Europe and North America. *Ecography* **38**: 321–329.

Suárez-Atilano M, **Burbrink F**, **Vázquez-Domínguez E. 2014**. Phylogeographical structure within *Boa constrictor imperator* across the lowlands and mountains of Central America and Mexico. *Journal of Biogeography* **41**: 2371–2384.

Sullivan BL, **Wood CL**, **Iliff MJ**, **Bonney RE**, **Fink D**, **Kelling S. 2009**. eBird: a citizen-based bird observation network in the biological sciences. *Biological Conservation* **142**: 2282–2292.

Tajima F. 1989. Statistical method for testing the neutral mutation hypothesis by DNA polymorphism. *Genetics* **123**: 585–595.

Tovilla-Sierra RD, **Herrera-Alsina LH**, **Bribiesca R**, **Arita HT. 2019**. The spatial analysis of biological interactions: morphological variation responding to the co-occurrence of competitors and resources. *Journal of Avian Biology* **50**: e02223.

Vásquez-Aguilar AA, **Ornelas JF**, **Rodríguez-Gómez F**, **MacSwiney-G MC. 2021**. Modeling future potential distribution of Buff-bellied Hummingbird (*Amazilia yucatanensis*) under climate change: species vs. subspecies. *Tropical Conservation Science* **14**: 1–18.

Vázquez-López M, **Córtes-Rodríguez N**, **Robles-Bello SM**, **Bueno-Hernández A**, **Zamudio-Beltrán LE**, **Ruegg K**, **Hernández-Baños BE. 2021**. Phylogeography and morphometric variation in the Cinnamon Hummingbird complex: *Amazilia rutila* (Aves: Trochilidae). *Avian Research* **12**: 61.

Velo-Anton G, **Parra JL**, **Parra-Olea G**, **Zamudio KR. 2013**. Tracking climate change in a dispersal-limited species: reduced spatial and genetic connectivity in a montane salamander. *Molecular Ecology* **22**: 3261–3278.

Venkatraman MX, **Deraad DA**, **Tsai WLE**, **Zarza E**, **Zellmer AJ**, **Maley JM**, **McCormack JE. 2019**. Cloudy with a chance of speciation: integrative taxonomy reveals extraordinary divergence within a Mesoamerican cloud forest bird. *Biological Journal of the Linnean Society* **126**: 1–15.

Warren DL, **Glor RE**, **Turelli M. 2010**. ENMTools: a toolbox for comparative studies of environmental niche models. *Ecography* **33**: 607–611.

Wei T, **Simko V. 2017**. *R package "corrplot": visualization of a Correlation Matrix (Version 0.84)*. Available at: https://github.com/taiyun/corrplot. Accessed 17 May 2020.

Wickham H. 2016. *ggplot2: elegant graphics for data analysis*. New York: Springer-Verlag.

Wiens JJ, **Graham CH. 2005**. Niche conservatism: integrating evolution, ecology, and conservation biology. *Annual Review of Ecology, Evolution, and Systematics* **36**: 519–539.

Zaldívar-Riverón A, **León Regagnon V**, **Nieto-Montes de Oca A. 2004**. Phylogeny of the Mexican coastal leopard frogs of the *Rana berlandieri* group based on mtDNA sequences. *Molecular Phylogenetics and Evolution* **30**: 38–49.

Zamudio-Beltrán LE, **Hernández-Baños BE. 2018**. Genetic and morphometric divergence in the Garnet-Throated Hummingbird *Lamprolaima rhami* (Aves: Trochilidae). *PeerJ* **6**: e5733.

Zamudio-Beltrán LE, **Licona-Vera Y**, **Hernández-Baños BE**, **Klicka J**, **Ornelas JF. 2020a**. Phylogeography of the widespread white-eared hummingbird (*Hylocharis leucotis*): preglacial expansion and genetic differentiation of populations separated by the Isthmus of Tehuantepec. *Biological Journal of the Linnean Society* **130**: 247–267.

Zamudio-Beltrán LE, **Ornelas JF**, **Malpica A**, **Hernández-Baños BE. 2020b**. Genetic and morphological differentiation among populations of the Rivoli's Hummingbird (*Eugenes fulgens*) species complex (Aves: Trochilidae). *The Auk* **137**: ukaa032.

Zarza E, **Reynoso VH**, **Emerson BC. 2008**. Diversification in the northern Neotropics: mitochondrial and nuclear DNA phylogeography of the iguana *Ctenosaura pectinata* and related species. *Molecular Ecology* **17**: 3259–3275.

Zink RM, **Barrowclough GF. 2008**. Mitochondrial DNA under siege in avian phylogeography. *Molecular Ecology* **17**: 2107–2121.

SUPPORTING INFORMATION

Additional supporting information may be found in the online version of this article on the publisher's website:

Table S1. Geographical information, number of genetically analysed samples (*N*) for mitochondrial DNA (*ND2* and *ATPase* 6 and 8) and number of distinct haplotypes (H) found in 15 *Amazilia yucatanensis* localities sampled in this study, with the number of individuals per haplotype in parentheses. Codes are from networks in Figure 2.
Table S2. Number of genetically analysed samples (*N*) and number of distinct haplotypes found in *Amazilia yucatanensis* individuals for mitochondrial DNA (*ND2* and *ATPase*) sampled by locality, with the number of individuals per haplotype in parentheses.
Table S3. Results of AMOVA and SAMOVA models on *Amazilia yucatanensis* populations, with data from locations with fewer than three samples removed from analyses.
Table S4. Pairwise comparisons of F_{ST} values among *Amazilia yucatanensis* populations.
Table S5. Contributions of the first two PCA-env axes to environmental space.

Figure S1. Haplotype median-joining networks of single *ND2* (A) and *ATPase* (B) data and combined *ND2* + *ATPase* data (C) for *Amazilia yucatanensis*.

Figure S2. Mismatch distributions (A) and Bayesian skyline plots (B) showing historical demographic trends for *Amazilia yucatanensis* subspecies *(Amazilia yucatanensis yucatanensis, Amazilia yucatanensis cerviniventris* and *Amazilia yucatanensis chalconota*) and for the whole species using mitochondrial sequences. Dashed lines correspond to observed frequencies of pairwise nucleotide differences, and continuous lines represent the expected frequencies under a sudden expansion model. Along the *y*-axis of the skyline plots is the population size estimated in units of $N_e\mu$ (N_e is effective population size and μ is the mutation rate per haplotype per generation). The *x*-axis is calendar time converted to thousands of years before present using a geometric mean substitution rate of 0.01214 s/s/l/Myr (Lerner *et al.*, 2011). Continuous lines represent median estimates, and shaded areas represent 95% confidence intervals. Population codes and font colours are as in Figure 1 and the Supporting Information (Table S1).

Figure S3. A, the contribution of the climatic variables on the two axes of the PCA-env and the percentage of inertia explained by the two axes (PC1 and PC2). B–J, histograms show simulated niche overlaps (grey bars) and the observed niche overlap between groups (bars with a circle) on which tests of niche equivalency (B–D) and niche similarity (E–J) were calculated from 100 iterations. The significance of the tests is shown. Abbreviations: CER, *Amazilia yucatanensis cerviniventris*; CHA, *Amazilia yucatanensis chalconota*; E_, niche equivalency; S_, niche similarity; YUC, *Amazilia yucatanensis yucatanensis*.